VATNAJÖKULL: Mass balance, meltwater drainage and surface velocity of the glacial year 2009_10

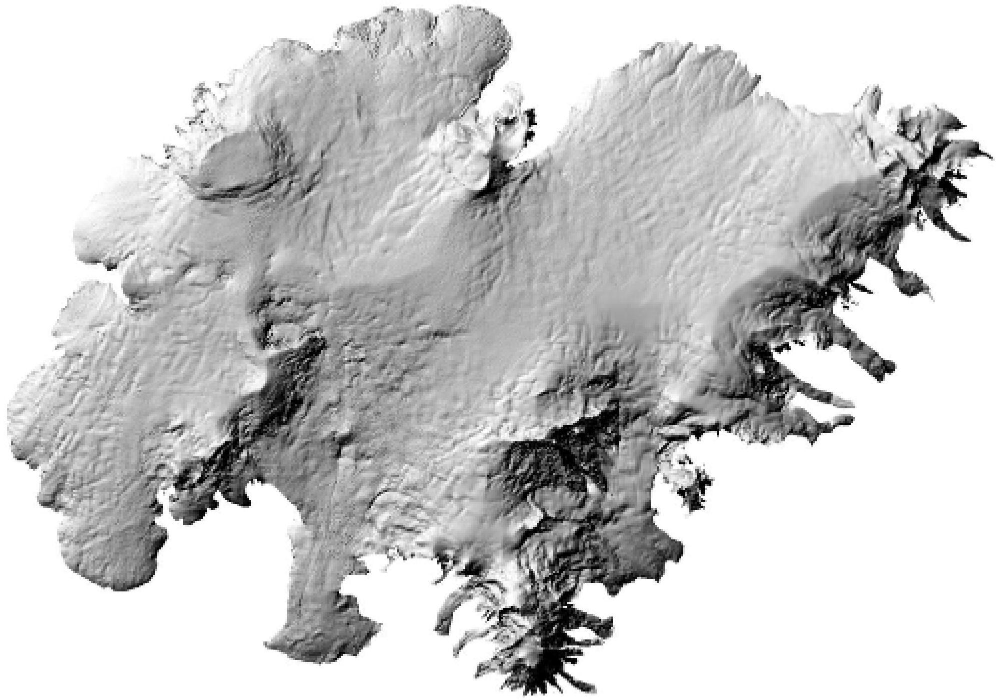

Institute of Earth Sciences
University of Iceland
and
National Power Company

Finnur Pálsson
Helgi Björnsson
Sverrir Guðmundsson
Hannes H. Haraldsson

RH-27-2013

Contents:

Figures:

Tables:

Appendixes:

1. INTRODUCTION

In 1992 (glacial year 1991_1992) a program of mass balance measurements was started for Vatnajökull by the Science Institute University of Iceland (now Institute of Earth Sciences, IES) in collaboration with the National Power Company (NPC). For the first year the program was limited to the western part of the glacier, but then expanded to include the northern outlets as well. In 1996 this study was further expanded to include southern outlets, with support from The European Union (Framework IV - Environment and Climate, TEMBA project 1996-1997). This program was extended 1998–2000 with further support from EU (Framework IV - Environment and Climate, ICEMASS project, 1998-2000). In 2000-2002 NPC and IES continued the program. In 2003-2005 IES participated in a multinational research project, which was financially supported by The European Union (EVK2-CT-2002-00152 SPICE). IES was responsible for obtaining data sets for calibration of models of the mass balance and dynamics of Vatnajökull. This work was also supported by The National Power Company of Iceland and The National Road Authority, and is a continuation of the TEMBA-project of 1996-97 and ICEMASS project 1998-2001.

In 2008-2009 IES and NPC continued a similar program. Mass balance measurements on the southeast outlets Breiðamerkurjökull and Hoffellsjökull is financially supported by the National Road Authority.

The aim of the collaborative work of NPC and IES is to improve our understanding of the mass balance and melt water runoff from glaciers. This work in combination with energy balance measurements by NPC and IES on Vatnajökull will be used for calibration of models of the energy and mass balance of Vatnajökull.

This report describes the field measurements and the initial results, the mass balance and melt water runoff for the glacial year 2009_10.

2. DIARY

January 29-30: mass balance measurements, set up of new ablation wires on Breiðamerkurjökull and Hoffellsjökull.
February 13-14: GPS survey of sites on Tungnaárjökull.
May 4 - 11: measurements of the winter balance.
June 5 - 10: measurements of the winter balance.
July 7: mass balance wires on Breiðamerkurjökull measured.
January 29-30: mass balance measurements, maintenance of AWS on Breiðamerkurjökull and Hoffellsjökull.
October 6 - 12: summer balance measurements.
October 13 mass balance measurements, set up of new ablation wires on Breiðamerkurjökull.

In all expeditions and short visits to the glacier the locations of mass balance stakes were measured with Kinematic GPS (or fast static GPS and a few with DGPS) for surface velocity calculation.

The following members of staff of the Institute of Earth Sciences, University of Iceland, carried out the fieldwork on Vatnajökull: Finnur Pálsson, Þorsteinn Jónsson, Sveinbjörn Steinþórsson, Eyjólfur Magnússon and Björn Oddsson. Also Hannes H. Haraldsson and Andri Gunnarsson (National Power Company) and Hlynur Skagfjörð Pálsson (Reykjavík Rescue Team). Members of the Iceland Glaciological Society, as well as members of Reykjavík, Hafnarfjörður Rescue Teams assisted in the fieldwork.

3. MASS BALANCE MEASUREMENTS

The purpose of the mass balance measurements is to describe the temporal and spatial distribution of the components of the mass balance. The mean annual values of the components and their variation from year to year are analyzed and related to meteoro-logical conditions and climatic variability. The results will be used in studies of changes in the glacier volume, estimates of meltwater contribution to glacial rivers, mass balance modeling, evaluation of altitudinal and regional variations of mass balance in response to climatic variations, and to assess the hydrometeorological and dynamic response of the ice cap to climate change.

The mass balance was determined by a stratigraphic method, measuring changes in thickness and density relative to the summer surface. The winter balance was estimated by drilling ice cores through the winter layer in the spring. Ablation was monitored from markers; snow stakes were put up on the glacier and wires were drilled down in the ablation area. The summer balance was measured in the autumn.

3.1 Methods

Measurements of the surface mass balance on a large ice cap like Vatnajökull are impractical in terms of cost with conventional techniques and sampling density that are typically used on small glaciers. The spatial variability of the mass balance may, however, be predictable on the flat large outlets of such an ice cap given data on several profiles extending over the elevation range of the glacier. The precipitation generally increases with elevation and decreases with the distance from the coast, but both the distribution of snowfall and redistribution of snow by drift depend on the prevailing wind direction during the winter. The summer melting depends mainly on the altitude and the albedo of the glacier surface. Therefore, we have used observations along a limited number of flowlines, which span the elevation range of the outlets to assess aerial estimates of surface mass balance. Each profile describes the variation with elevation, but together they also describe the lateral variation of the mass balance. Recently, modern over-snow vehicles and helicopters have allowed fast traverses to ensure successful fieldwork in spite of frequently poor weather conditions. Error limits for the area integrals of the mass balance components must nevertheless be within 15%.

The winter mass balance (b_w) is defined as the mass of snow accumulated during the winter months, the summer balance (b_s) is the mass balance during the summer, and the net balance (b_n) is defined as their sum. The specific mass balance is expressed in terms of the equivalent thickness of water. All mass balance components apply to a time interval between given measurement dates, which are not fixed from one year to another. The dates in the autumn are separated by approximately one calendar year, which roughly coincides with the glaciological year defined as October 1st to September 30th. Snow cores are drilled in April-May through the winter layer and profiles of the density are measured. The summer balance is derived in the autumn from measurements of the changes in the snow core density during the summer in the accumulation area and from readings at stakes and wires drilled into the ice in the ablation areas.

Digital maps are created for winter, summer and net balance for the whole ice cap based on site measurements. The mass balance is calculated over both the ice and water drainage basins. The summer balance over the water basin is an estimate of meltwater contribution to rivers and groundwater storage. This estimate, however, does not include precipitation that falls as rain on the glacier nor snow, which falls and melts during the summer. The meltwater contribution is compared with river runoff at stream flow gauges closest to the glacier. For this comparison, we define the glaciological year from the start of October to the end of September and the period draining meltwater from the glacier during the summer from June through September. It would be misleading to include May in the summer period because runoff from the glacier melt in May is delayed due to refreezing during elimination of the cold wave.

3. 2 Results of mass balance measurements.

Mass balance measurements were done at 57 sites in spring 2010 (Fig. 1). The specific mass balance at individual sites is shown in Fig. 2. Most sites are on central flow lines at individual outlets. The specific mass balance along flow lines is given in Fig. 3 as a function of elevation for each glacier outlet: Síðujökull, Tungnaárjökull, Dyngjujökull, Köldukvíslarjökull, Brúarjökull (west and east), Eyja-bakkajökull, Hoffellsjökull and Breiðamerkurjökull.

Digital maps for winter, summer and net balance are shown in Figure 4. Although no balance measurements are available for Skeiðarárjökull, the balance has been estimated by interpolating the balance values from the neighboring outlets, based on our experience from previous years. The mass balance of individual large outlets is discussed in the following subsections. A DEM of Vatnajökull showing the surface of ca. 2010, is the base for all area distributions and delineation of ice drainage basins.

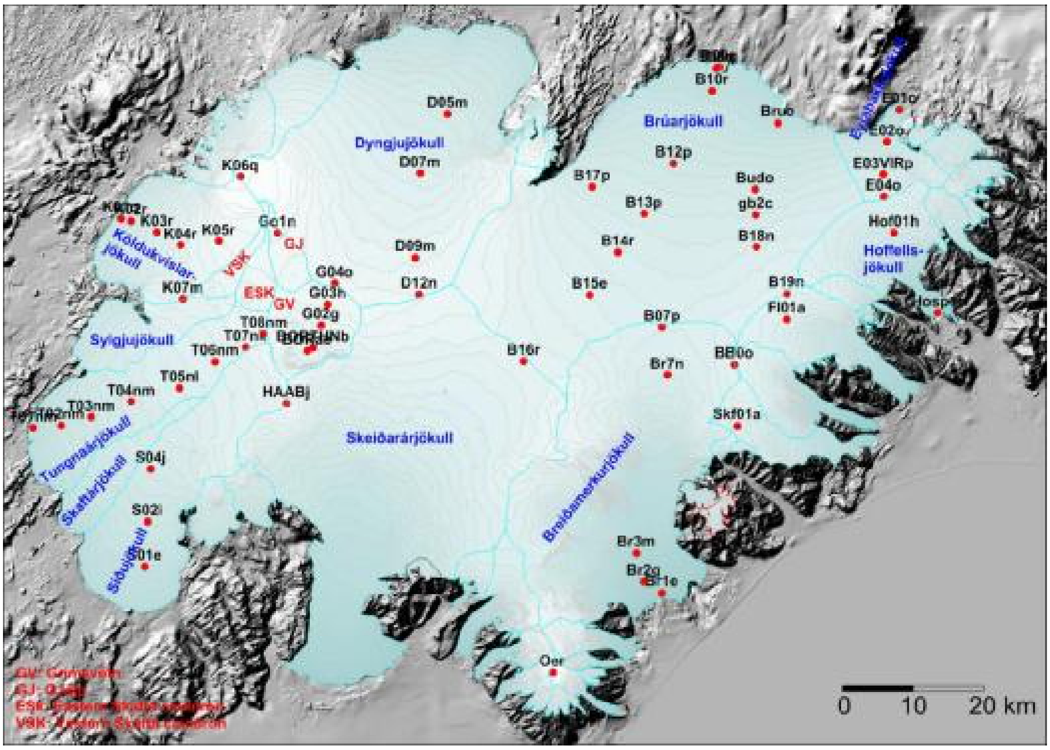

Figure 1. Outlets of Vatnajökull and location of mass balance measurement sites 2009_10. At blue points only summer ablation was measured.

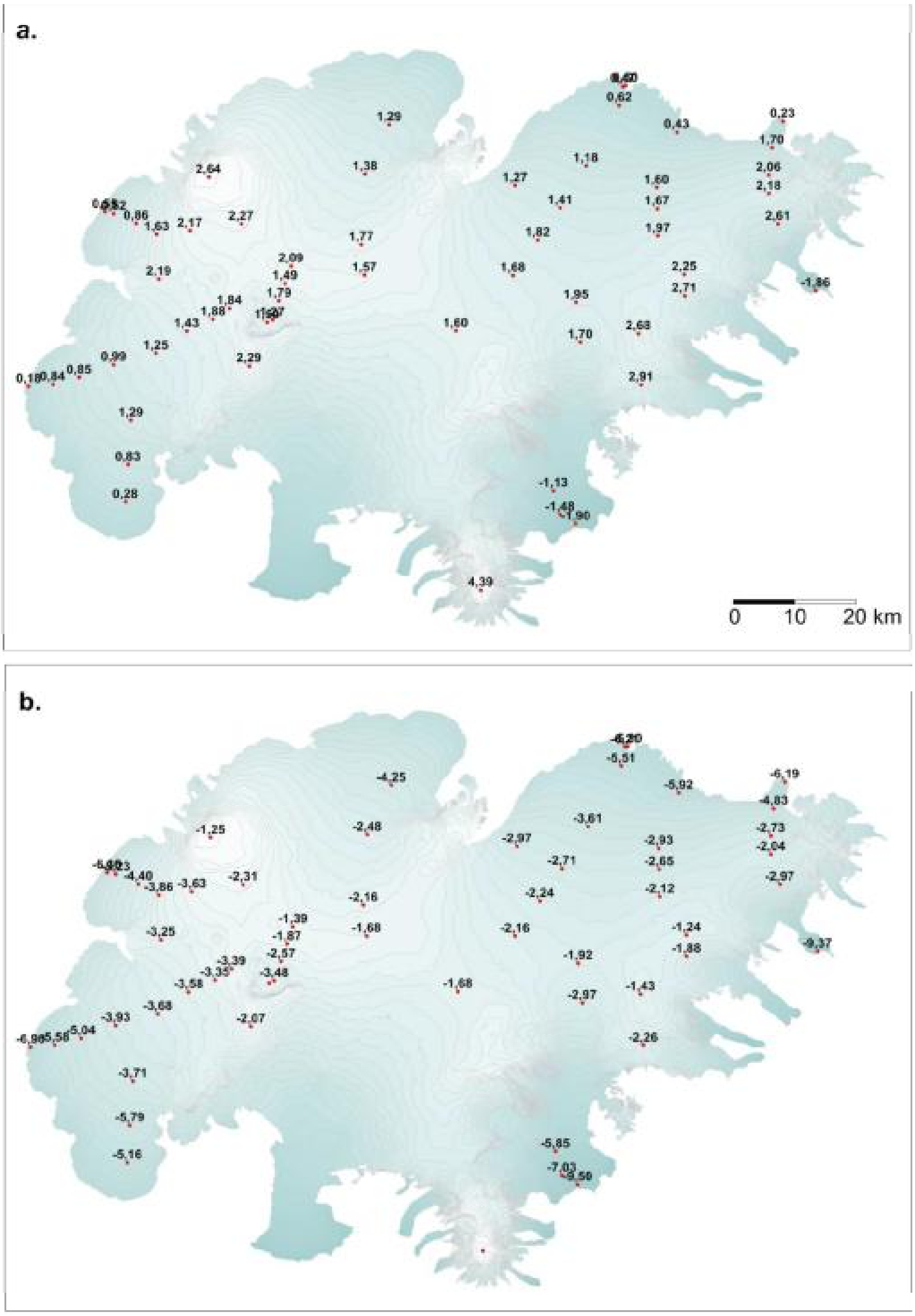

Figure 2. a. Map showing point values of specific winter mass balance in m water equivalent (m_{we}), 2009_10. b. Map showing point values of specific summer balance in 2010.

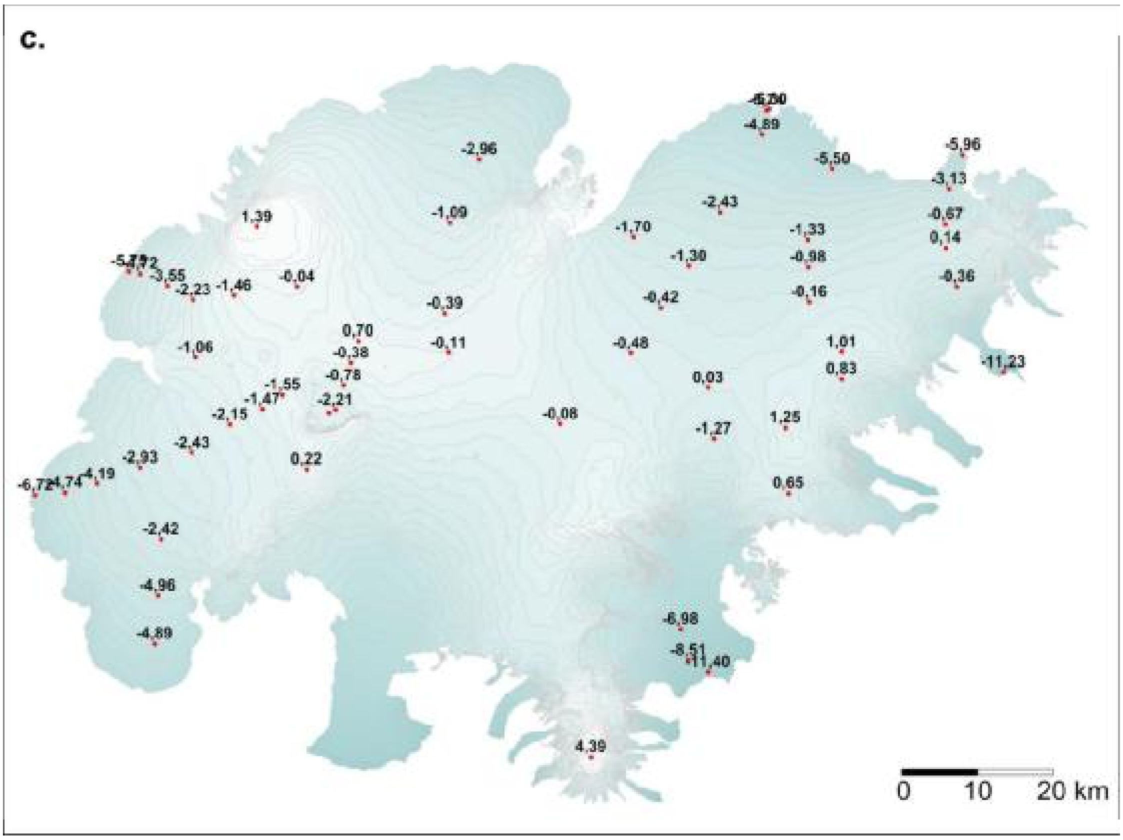

Figure 2. c. Map showing point values of specific net mass balance (m_{we}), 2009_10.

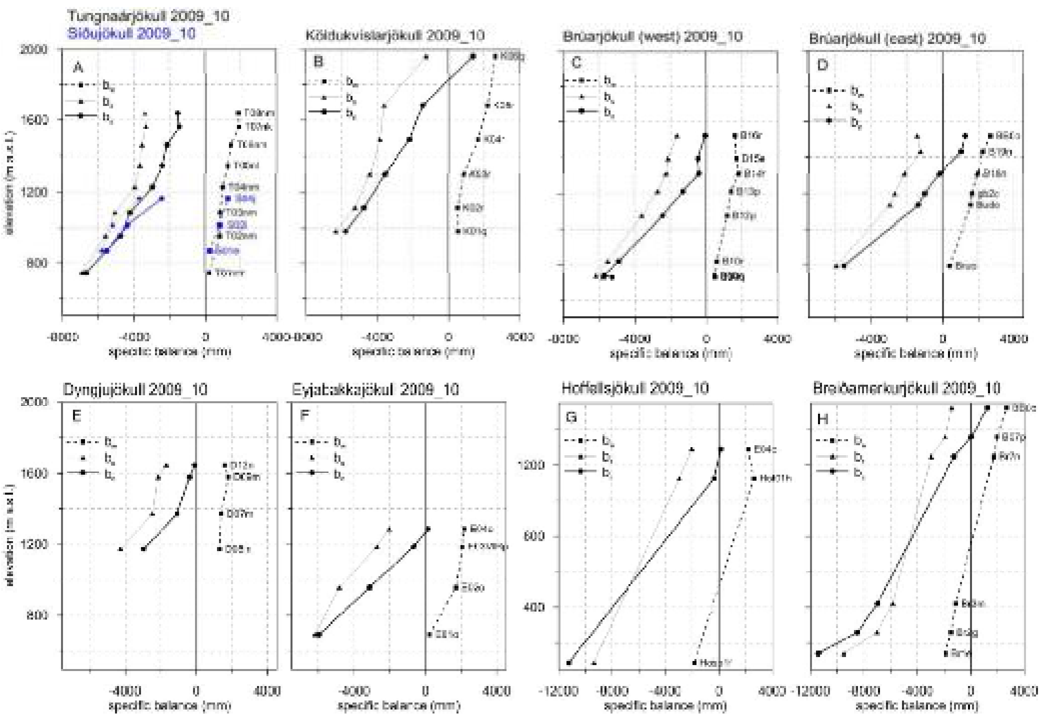

Figure 3. Mass balance 2009_10 as a function of elevation on central flow lines on Vatnajökull outlets.

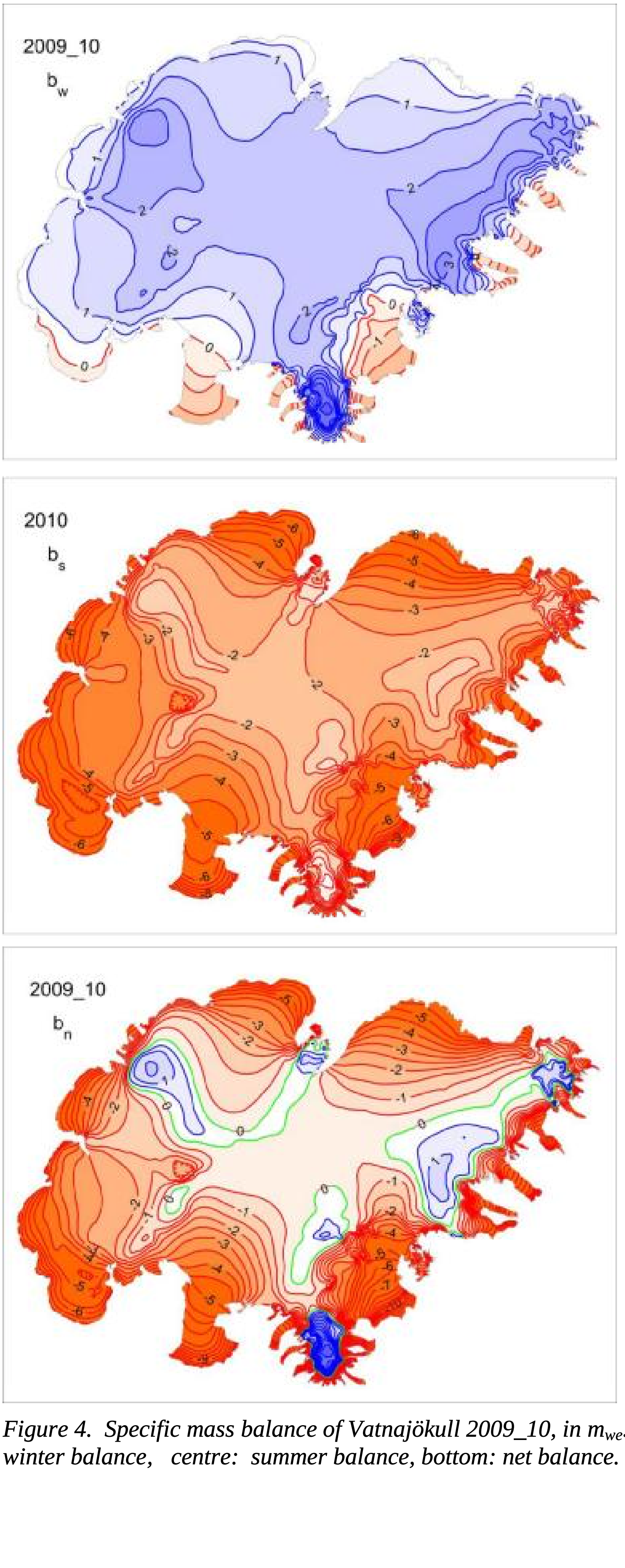

Figure 4. Specific mass balance of Vatnajökull 2009_10, in m_{we}. Top: winter balance, centre: summer balance, bottom: net balance.

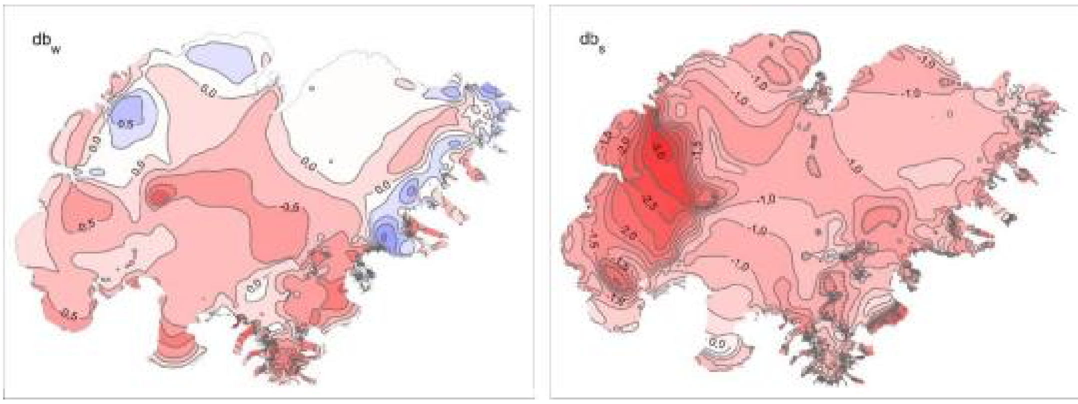

Figure 5. The left frame shows the difference between winter balance in 2009_10 and the average winter balance 1995_96 to 2008_09. (Positive (blue) is higher than average). The left frame shows the difference between summer balance in 2010 and the average summer balance 1996 to 2009. (Negative (red) is higher than average ablation).

The winter 2009_2010 was warm in Iceland, and also exceptionally dry. Very little snow accumulated in lowland areas. For long periods of the winter a high pressure system over Iceland diverted the North Atlantic low pressure systems south of Iceland. This is reflected in extremely low snow accumulation in most of Vatnajökull. (fig. 5, see also Appendix F, MODIS image series for the winter).

The summer 2010 was exceptionally warm (in SW Iceland, the warmest in surveyed records, close to the extremely warm summers in the 1930´s). Most summer was also dry, especially in SW Iceland. (Information about weather is from the web site of the Iceland met office written by Trausti Jónsson). Inspection of the MODIS monthly overview of the summer months in Appendix F show that days with clear skies over Vatnajökull were 6 in the latter half of May, ~13 in June, ~14 in July, ~12 August and ~5 in first half of September.

Tephra from the eruption plume in the last days of the Eyjafjallajökull eruption was brought over Vatnajökull (see MODIS images for May and early June in appendix F); large quantities settled on the snow surface on W-Vatnajökull. In addition to the sparse tephra deposited on E-Vatnajökull we assume that relevant quantities of dust were blown over the glacier from the snow free northern highland, mostly later in June and July. The tephra and dirt abruptly lowered the albedo. The dry, often clear sky, period that followed resulted in extreme ablation especially in the western accumulation zone, where almost no ablation would have been without tephra. This enhanced melt continued the whole summer in the accumulation zones where the tephra particles stay in the surface. In the ablation zones most of the snow melted and washed away in a record time due to the low albedo, but the tephra particles where washed away soon as the snow-cover had melted. However the bare ice (low albedo) was exposed and enhanced melting continued. The summer ablation was extreme at survey sites, but most extreme in the accumulation areas of Köldukvíslarjökull, Tungnaár-jökull, Sylgjujökull, and the water catchments of Skaftárkatlar and Grímsvötn.(see MODIS images for late May and June in appendix F. All this resulted in extreme ablation (see fig. 5) on all of Vatnajökull.

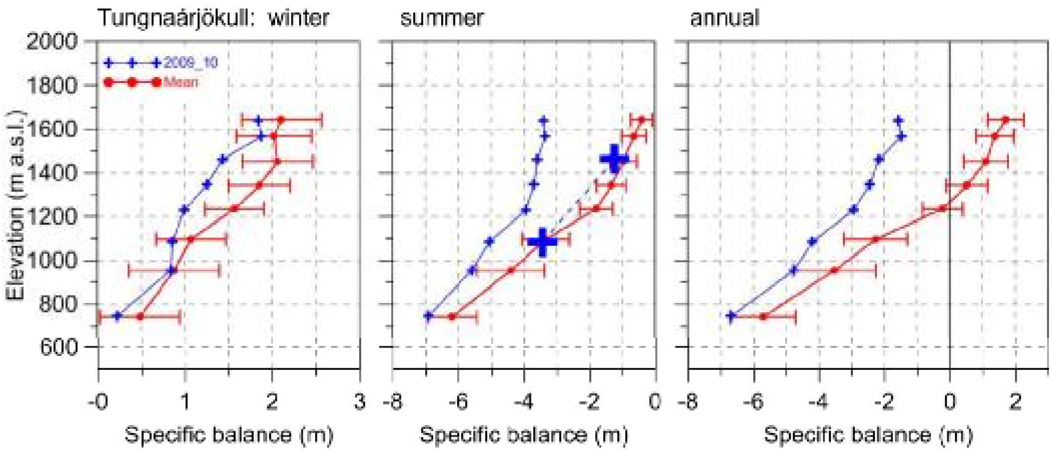

Figure 6. Mass balance at a central flow line of Tungnaárjökull 2009_10, and average mass balance 1991_92 to 2008_09. The thick blue + show estimates of ablation at two automatic weather stations if no tephra had been deposited (Sverrir Guðmundsson pers. com.).

3.2.1 Tungnaárjökull.

Area = 345 km^2
B_w= 0.37 km^3 ; b_w = 1.07 m
B_s = -1,56 km^3 ; b_s = -4.53 m
B_n = -1,19 km^3 ; b_n = -3.46 m
ELA = above highest elevation
AAR = 0 %

(The terms are defined at the foot of this page)

Variation of mass balance along a central flow line on Tungnaárjökull is shown in Fig. 6. The winter balance was extremely low at most survey sites, in total only 73% the 1991_92-2008_09 average. In May fine grained tephra from the Eyjafjallajökull eruption was deposited on the surface. The tephra effectively lowered the albedo and high ablation rates were observed everywhere on the outlet. The warm and often cloud-free summer further enhanced ablation. Energy balance estimates from AWS data suggest that without tephra deposits, ablation would have been close to average (Sverrir Guðmundsson). Extreme ablation was observed at all survey sites, ablation in areas above 1200 m was almost independent of elevation. The summer ablation was 82% over average. The net balance was negative the 17th year in a row, the mass loss 3.3 times that of an average year during the survey period.

3.2.2 Köldukvíslarjökull

Area = 301 km^2
B_w = 0.42 km^3 ; b_w = 1.39 m
B_s = -1.25 km^3 ; b_s = -4.15 m
B_n = -0.83 km^3 ; b_n = -2.76 m
ELA = 1830 m (at profile)
AAR = 8 %

Variation of mass balance along a central flow line on Köldukvíslarjökull is shown in Fig. 7. Winter balance was much higher than average in the upper accumulation zone, but far lower than average in blow ~1300m. In spite of abnormal distribution of the winter snow, the total winter balance was 97% of average since 1991_92. The tephra from Eyjafjallajökull was deposited on Köldukvíslarjökull in May, especially in an area north of the Skaftár cauldrons and west of the Gjálp eruption site, in the accumulation zone. Ablation was extreme at all survey sites especially above 1200 m elevation. The total summer ablation was 2.25 fold that of an average summer. The net balance was negative the 16th year in a row, the mass loss was seven-fold that of an average year during the survey period.

B_w,B_s and B_n are water equivalent volumes of winter, summer and net balance, ELA the equilibrium line altitude, and AAR is the accumulation area ratio.

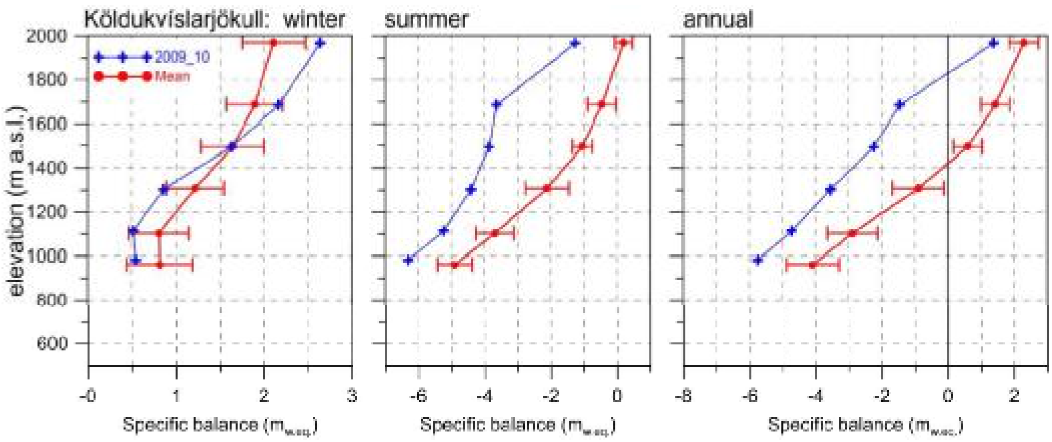

Figure 7. Mass balance at a central flow line of Köldukvíslarjökull 2009_10, and average mass balance 1991_92 to 2008_09.

3.2.3 Dyngjujökull

Area = 1064 km^2
B_w= 1.52 km^3 ; b_w = 1.52 m
B_s = -3.14 km^3 ; b_s = -2.95 m
B_n = -1.52 km^3 ; b_n = -1.43 m
ELA = 1675 m (at profile)
AAR = 24 %

Variation of mass balance along a flow line on Dyngjujökull is shown on Fig. 8. The winter balance in 2009_10 was close to average at 1400 m, higher than average at the lowest site, extremely low at the higher sites. In total the winter balance was at average.

The summer ablation was extreme at all survey sties, some is explained by tephra from Eyjafjallajökull, but the summer was also warm and sunny. The total summer balance was twofold that of an average year. The net balance was highly negative, -1.43 m, while the average is close to zero.
Mass balance was not measured at the lowest elevations, but assumed to be similar (as a function of elevation) to that of Brúarjökull and Köldukvíslar-jökull.

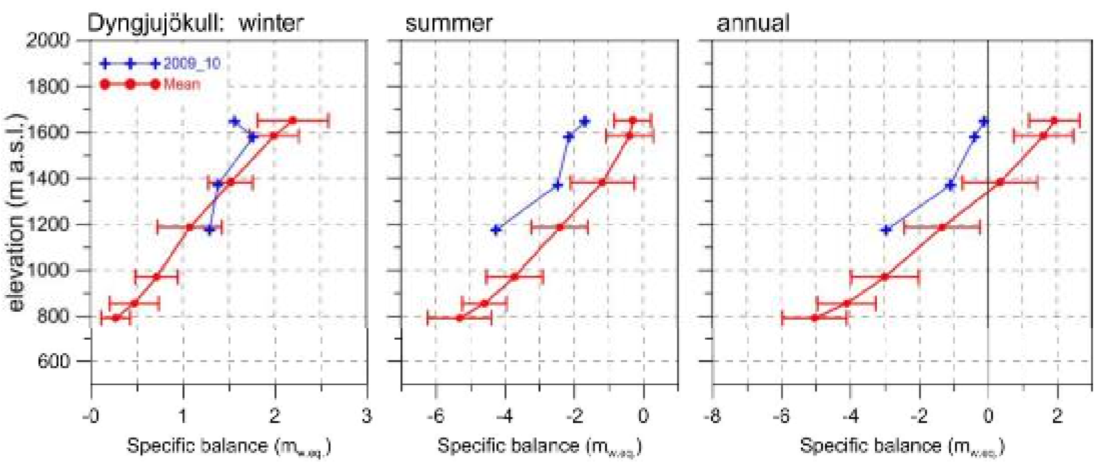

Figure 8. Mass balance at a central flow line on Dyngjujökull 2009_10, and average mass balance 1991_92 to 2008_09 (except 1998_99 – 2003_04 at all but the top elevation).

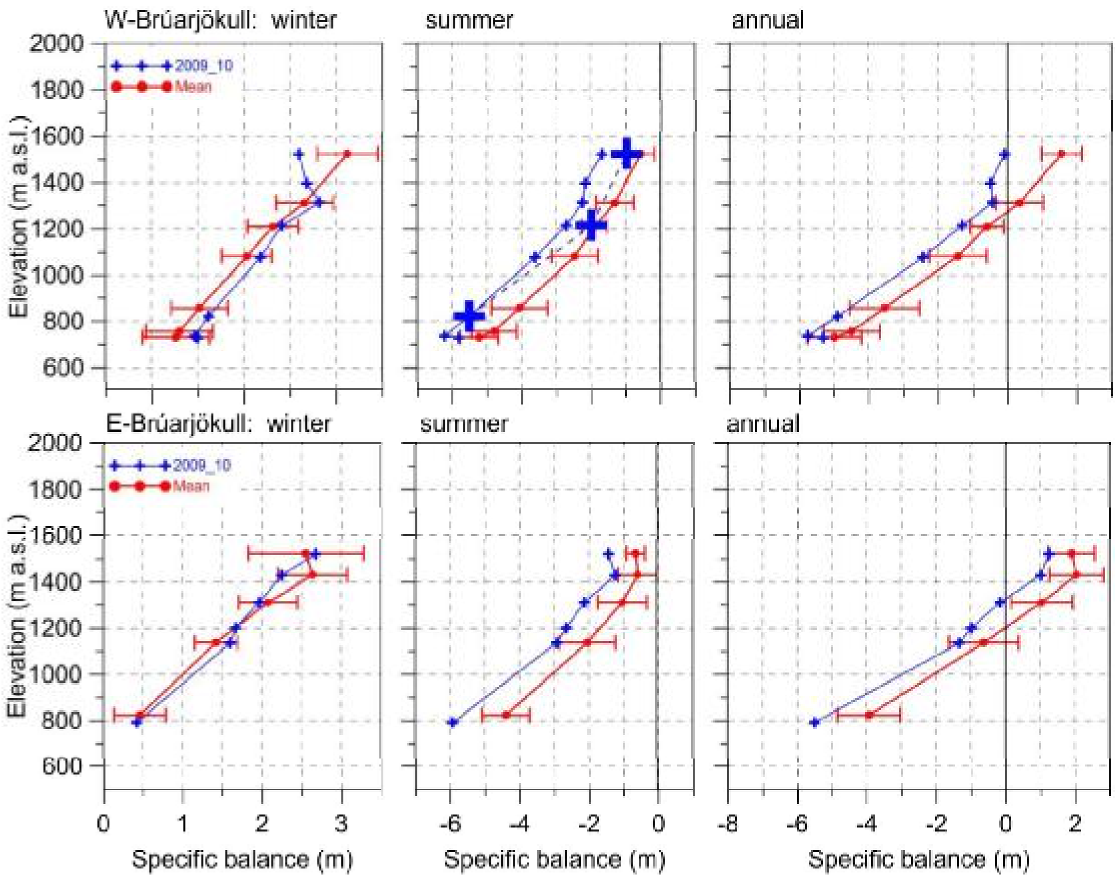

Figure 9. Mass balance at two flow lines on Brúarjökull 2009_10, and average mass balance 1992_93 to 2008_09. The thick blue + show estimates of ablation at three automatic weather stations if no tephra had been deposited (Sverrir Guðmundsson).

3.2.4 Brúarjökull

Area = 1526 km^2
B_w= 2.28 km^3 ; b_w = 1.49 m
B_s = -4.41 km^3 ; b_s = -2.89 m
B_n = -2.13 km^3 ; b_n = -1.40 m
ELA = 1545 m (western flow line)
ELA = 1325 m (eastern flow line)
AAR = 14 %

Variation of mass balance along two flow lines on Brúarjökull is shown on Fig. 9. The winter balance close to average at most survey sites. However above 1400 m on the western profile accumulation was much less than average, and general accumulation lowers towards west. In total the winter accumulation was close to average. Some tephra from Eyjafjallajökull was deposited in accumulation area of Brúarjökull, but very little if any on the ablation zone. This, together with a warm and sunny summer, resulted in extreme ablation. The surface energy balance for three AWS's at sites on the western profile was modelled with and without the effect of the tephra cover on surface albedo. The model results suggest that without the tephra ablation in the accumulation would be slightly over average, while ablation in the ablation zone would have been similar. The total ablation was about 50% more than average. The net balance was negative, the 13ht year of the 18 year survey period. The mass loss was 3.5 fold that of an average year.

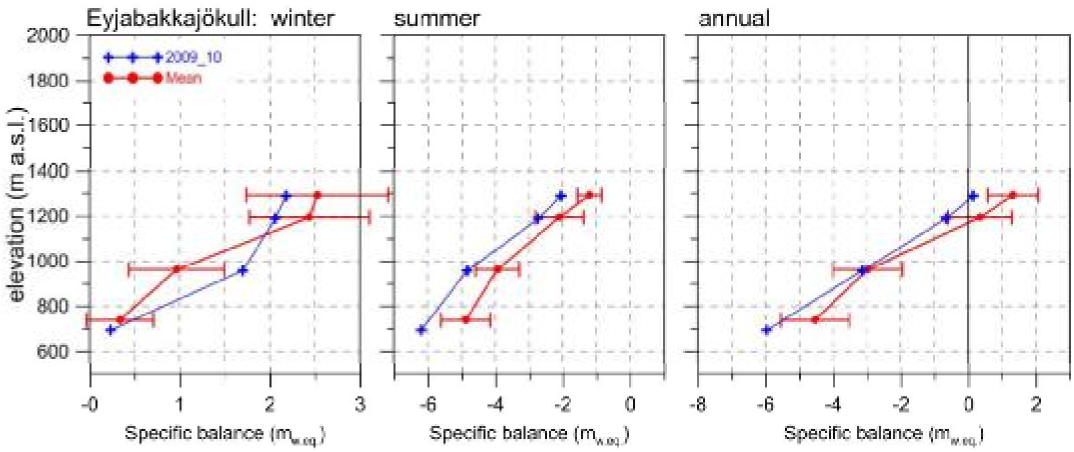

Figure 10. Mass balance at a central flow line of Eyjabakkajökull 2009_10 and average mass balance 1995_96 to 2008_09.

3.2.5 Eyjabakkajökull

Area = 113 km^2
B_w= 0.21 km^3 ; b_w = 1.84 m
B_s = -0.38 km^3 ; b_s = -3.39 m
B_n = -0.17 km^3 ; b_n = -1.55 m
ELA = 1270 m (at profile)
AAR = 18 %

Variation of mass balance along a central flow line on Eyjabakkajökull is shown on Fig. 10. Winter balance was higher than average in the mid and elevation range but much lower than average at the upper survey sites. In total the winter balance was 10% over the average. In the warm and sunny summer ablation was less far over average at all survey sites (there are no indication of tephra from Eyjafjallajökull in this part of Vatnajökull). The summer ablation was 40% over the average. The net balance was negative, the mass loss more than twofold that of an average year since 1995_96.

3.2.6 Breiðamerkurjökull

Area = 938 km^2
B_w= 0.89 km^3; b_w = 0.95 m
B_s = -3.33 km^3 ; b_s = -3.54 m
B_n = -2.44 km^3 ; b_n= -2.59 m
ELA = 1355 m (at profile)
AAR = 16 %

Variation of mass balance along a central flow line on Breiðamerkur-

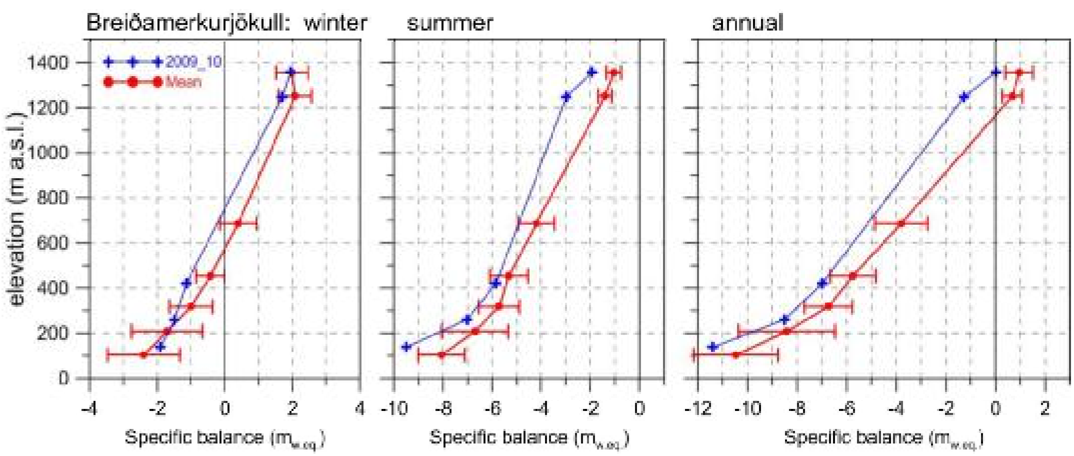

Figure 11. Mass balance at a central flow line of Breiðamerkurjökull 2009_10, and average mass balance 1995_96 to 2009_10.

jökull is shown on Fig. 11. Snow accumulation was close to average in the upper area, less than average in the mid elevation range and winter ablation was close average at the lowest sites. The winter balance was only ~70% of the average. Ablation was much higher than average at all survey sites, summer was warm and sunny. The summer ablation was 1.4 times the average. The net balance was negative, the mass loss twofold that of an average year since 1995_96.

3.3 The mass balance record for Vatnajökull.

From the digital maps the total volumes of winter, summer and net balance have been calculated by integration (appendix D, gives balance values as a function of elevation) and are as follows:

$$\mathbf{B_w = 10.50\ km^3\ ;\ b_w = 1.32\ m}$$
$$\mathbf{B_s = -26.50\ km^3\ ;\ b_s = -3.33\ m}$$
$$\mathbf{B_n = -16.00\ km^3\ ;\ b_n = -2.01\ m}$$

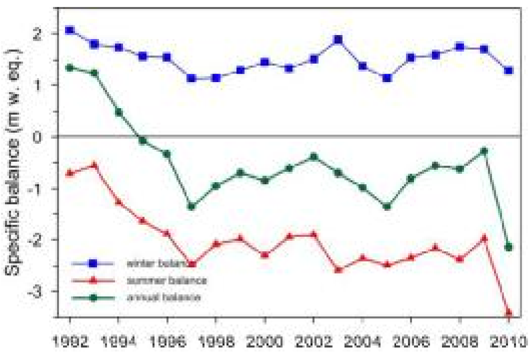

Figure 12. Specific mass balance of Vatnajökull 1991_92 – 2009_10.

The warm and dry winter conditions to lower than average winter balance by 15% (over the observation period 1991_92-2008_09, Fig. 12). The 0 mass balance turnover for Vatnajökull (current topography) is close to 13.4 km^3 (1.64 m w. eq.) and the winter balance 2009_10 is 80% of that. The summer was extremely warm and sunny and dry. This and tephra deposited on Vatnajökull in last days of the Eyjafjallajökull eruption in lead to extreme ablation on Vatnajökull, especially in the accumulation zones. The summer ablation was 1.7 fold that of an average summer over the survey period, two times higher than for zero balance turnover. Net balance was negative the 16th year in a row; the mass loss was almost threefold the average (-0.70 m) the past 15 consecutive years of negative balance.

The glacial year of 2009_10 was the 16th in a row with negative mass balance for Vatnajökull (Fig. 12, Fig. 13), contributing to a total loss of -12.5 m_{we} (ice volume of ~112 km^3) since 1994_95.

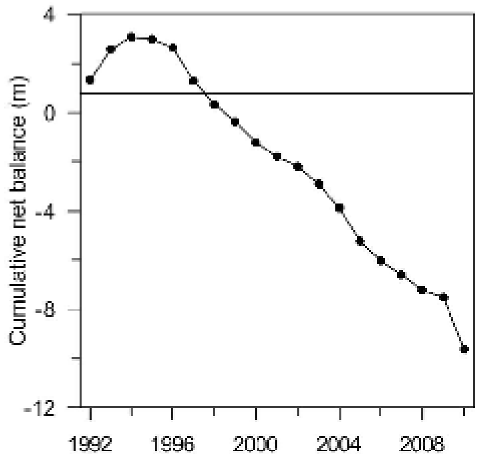

Figure 13. Cumulative specific mass balance of Vatnajökull 1991_92 – 2009_10.

The temporal variability of mass balance for different outlets is shown in Fig. 14. The greatest variability of the winter balance is for Eyjabakkajökull the eastern most of studied outlets. This part of the glacier is open to precipitation from all south- and east- and north-easterly wind directions, and thus has high snow accumulation in winters when the paths of the North Atlantic lows is just east of Iceland. This is also the case for the eastern part of Brúarjökull.

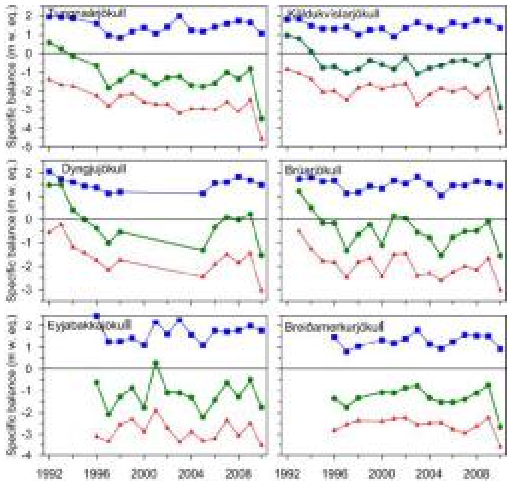

Figure 14. Specific mass balance of Vatnajökull outlets 1991_92-2009_10.

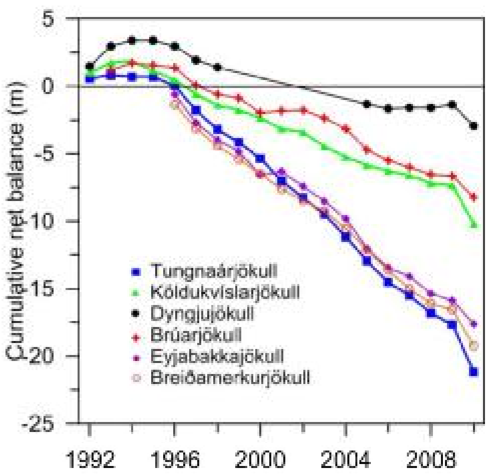

Figure 15. Cumulative specific mass balance for several of Vatnajökull outlets 1991_92 – 2009_10.

Breiðamerkurjökull shows lowest variability. It is a maritime glacier with climate controlled by the stable sea temperature and humid air mass. The longest winter balance records seem to reveal periodic behavior, with peaks in ~1991_92 and 2002_03 and a low in ~1998. The cumulative net balance curves for the outlets of Vatnajökull in Fig. 15 show that all outlets have been losing mass since 1994_95. The slope for mass loss is about 0.7 ma^{-1} for northern outlets but 1.5 ma^{-1} for the south and western outlets.

In Fig. 16 the relation of the annual net balance to the accumulation area ratio (AAR) and equilibrium line altitude (ELA) is shown for different outlets over the survey period. The b_n-AAR gradient is similar for all outlets, about 0.5 m_{we} for 10% change in AAR. The zero-balance AAR varies for different outlets from about 60-65%, similar for all outlets except for the southern outlet Breiðamerkurjökull.

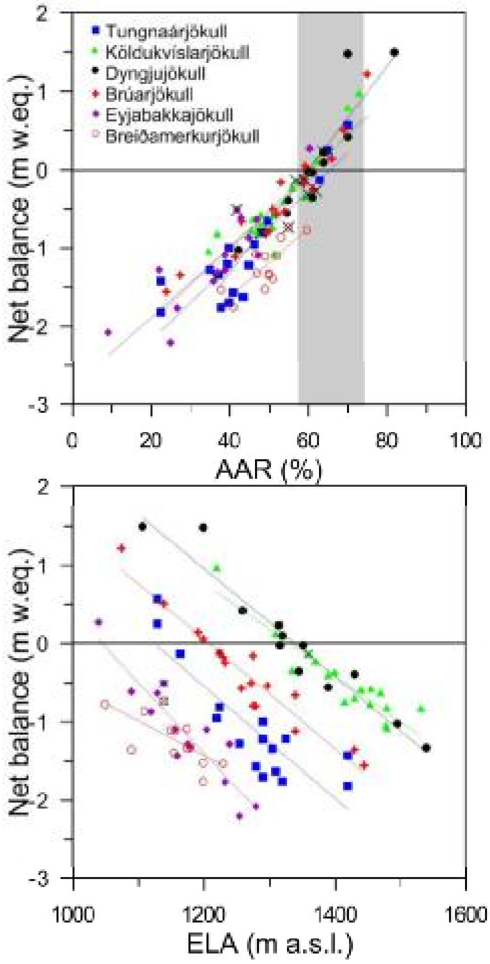

Figure 16. The relation between net annual balance (b_n) and accumulation area ratio (AAR)(upper) and b_n and equilibrium line altitude (ELA), for Vatnajökull outlets during the survey period. (This years points are marked with a black x).

Breiðamerkurjökull is far from equilibrium, the ablation area is too large. A large part of the glacier has carved 200-300 m through the former sediment bed, and the surface elevation has lowered accordingly. Breiðamerkurjökull is now retreating at a high rate.

Similarly the zero-balance ELA varies from about 1000-1100 m for the southern outlets to 1400 m for the NW outlets. The b_n-ELA slope is similar for all outlets -0.7 m w. eq. per 100 m.

4. SURFACE VELOCITY MEASUREMENTS

The surface velocity of the glacier was calculated from DGPS (accuracy within 1 m), fast static (accuracy about 1 cm) and kinematic GPS (accuracy about 3 cm) positioning of the ablation stakes. All sites were surveyed in spring and autumn (most kinematic, some DGPS), and many also in June (kinematic), August (fast static) and October (kinematic). At a few sites stakes from previous years were found and resurveyed, making it possible to calculate surface velocity over a year or longer time span. The average summer surface velocity is shown on Figure 17.

The use of more accurate instruments and setup, allows estimation of vertical as well as horizontal velocities. Two 6 metre long 4 inch metal poles where set up in the accumulation zone of the western outlet Tungnaárjökull and one on east Brúarjökul to directly measure the vertical displacement. Small GPS units are also attached to the poles and run continuously. At sites close to the glacier edge very small horizontal movement is measured. This indicates that the glacier snouts are almost stagnant. In the centre areas of some of the outlets especially close to the

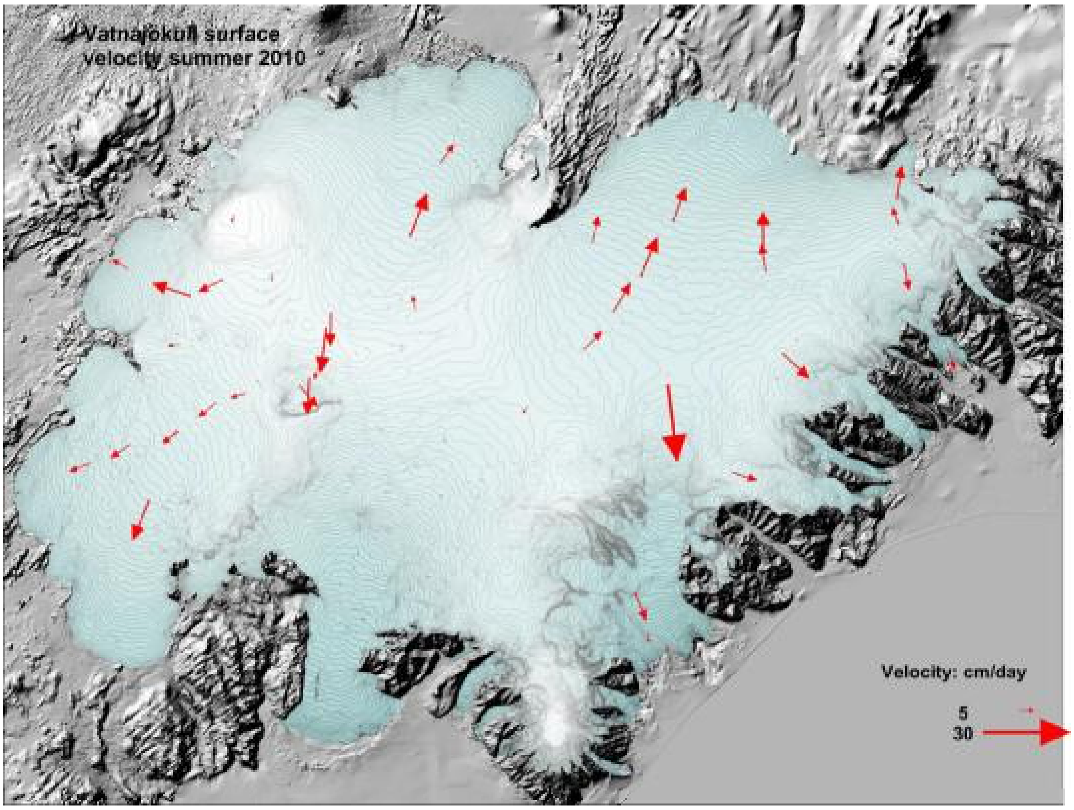

Figure 17. Average surface velocity during summer 2010.

equilibrium line, there is an increase in velocity during summer compared to winter. The summer velocity is of the order of two-fold the winter velocity. This suggests that basal sliding is increased in the melting season, and is of the same magnitude as the deformation velocity.

From previous velocity measurements, surging of outlets has been predicted. No signs of a starting surge are seen from this year's survey.

5. Melt water runoff.

draining melt water from Vatnajökull. The summer balance over the water basin is an estimate of meltwater contribution to rivers and groundwater storage. This estimate, however, does not include precipitation that falls as rain on the glacier, or snow, which falls and melts during the summer. The meltwater contribution can be compared with river runoff at stream-flow gauges closest to the glacier. For this comparison, we define the glaciological year from the start of October to the end of September and

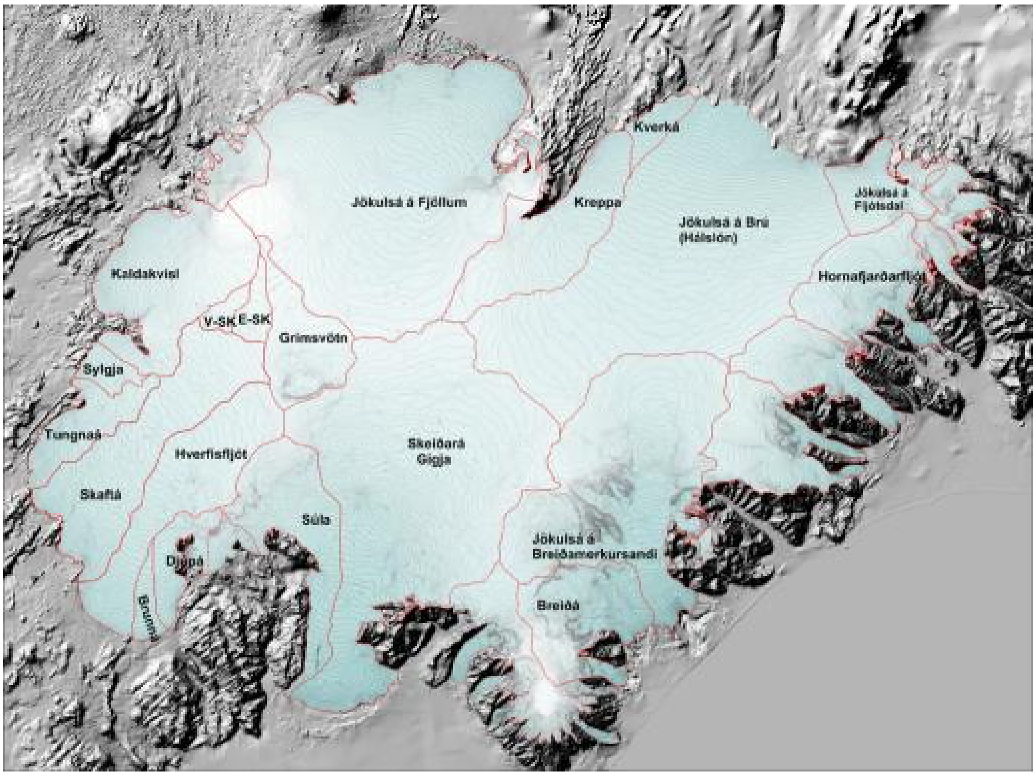

Figure 18. Water divides and drainage basins of selected rivers draining water from Vatnajökull.

Water divides and drainage basins for rivers draining water from Vatnajökull have been defined from water pressure potential maps. The potential maps were produced from existing surface for summer 2010 (from SPOT5 satellite images) and bedrock digital elevation models.

Figure 18 shows the water divides and drainage areas for selected rivers the period draining meltwater from the glacier during the summer from June through September. It would be misleading to include May in the summer period because runoff from the glacier melt in May is delayed due to refreezing during elimination of the cold wave and because of the contribution of the spring melt from the highlands to the runoff. Some

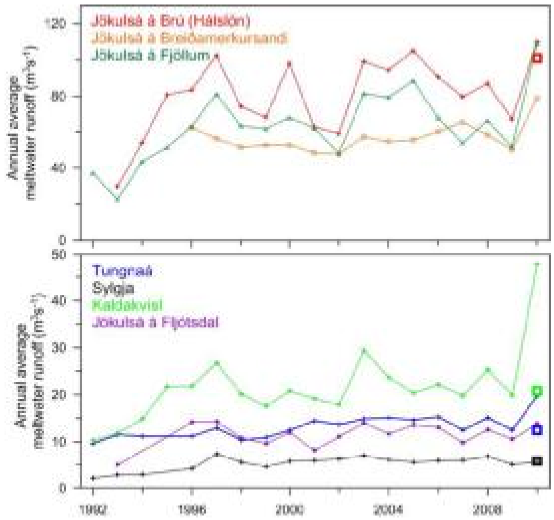

Figure 19. The temporal variation of the average annual meltwater runoff to different river catchments. The estimated runoff without the enhanced melt due to the tephra from Eyjafjallajökull is shown with thick rectangles (Sverrir Guðmundsson).

ablation also occurs during winter, especially in the low snouts of the southern outlets. Average melt water runoff to different rivers is given in Table I, and temporal variation of the average meltwater runoff in Fig. 19. The average specific runoff (q_s) differs from basin to basin from 99 to 182 $ls^{-1}km^{-2}$. This is mainly due to different elevation distributions, for example, the water drainage basins for Tungnaá and Kverká are within the ablation area, while that of Grímsvötn and Skaftárkatlar are high in the accumulation zone.

Water Catchment:	**Area (km^2)**	**ΣQ_s ($10^6 m^3$)**	**Q_s (m^3s^{-1})**	**Q_a (m^3s^{-1})**	**q_s ($ls^{-1}km^{-2}$)**
Vatnajökull	7968	26575	2521,1	842,7	105,8
Tungnaá	122	625	59,2	19,8	162,6
Sylgja	40	180	17,1	5,7	143,7
Kaldakvísl	368	1507	143,0	47,8	129,9
Jokulsa a Fjöllum	1188	3445	326,8	109,2	91,9
Kreppa	291	744	70,5	23,6	81,0
Kverka	47	245	23,2	7,8	165,2
Jokulsa a Brú	1215	3472	329,3	110,1	90,6
Jökulsá á Fljótsdal	131	436	41,4	13,8	106,0
Jökulsá í Lóni	101	332	31,5	10,5	103,9
Hornafjarðarfljót	239	779	73,9	24,7	103,3
Jökulsá á Breiðam	740	2492	236,4	79,0	106,9
Breiðá-Fjallsá	235	1025	97,2	32,5	138,5
Skeiðará-Gígja	1165	3434	325,8	108,9	93,5
Súla	256	990	93,9	31,4	122,7
Brunná	36	206	19,5	6,5	182,4
Djúpá	84	405	38,5	12,9	153,6
Hverfisfljót	318	1299	123,2	41,2	129,6
Skaftá	395	1776	168,5	56,3	142,6
Grímsvötn	173	444	42,1	14,1	81,2
Eystri Skaftárketill	39	123	11,7	3,9	99,0
Vestari Skaftárketil	25	88	8,3	2,8	110,8

ΣQ_s: total summer melt water; Q_s : average runoff (averaged over summer, 4 months, June – September)
Q_a : average runoff (averaged over a whole year); q_s : average runoff per km^2 (averaged over a whole year)

6. Conclusions

The winter 2009_10 was warm and dry. The summer was also warm and sunny The relatively long periods of clear skies, in the months of highest solar angle, combined with thin tephra cover from the Eyjafjallajökull eruption and dirt blown over the glacier in the dry periods in late May and June, enhanced ablation. This was most significant in the upper region of western Vatnajökull. All this resulted in exceptionally high ablation in all areas but most prominent in the accumulation areas northwest of Grímsvötn.
The winter balance (13.56 km^3) was lower than average by 15% (over the observation period 1991_92-2008_09). The extreme summer ablation (-26.50 km^3) was ~1.7fold that of an average summer during the survey period. The net balance was highly negative (-16.56 km^3), the mass loss was almost threefold the average (-0.70 m) of the past 15 consecutive years of negative balance. The accumulation area ratio was 46% for the total glacier.
The glacial year of 2011_12 was the 16th in a row with negative mass balance for Vatnajökull (since 1994_95) contributing to a total loss of 12.5 m_{we}, 0.79 $m_{we}a^{-1}$ or an average surface lowering of 0.88 ma^{-1}. This is equivalent to a total ice volume of ~112 km^3, or ~3.7% loss off the total ice mass of Vatnajökull.

Summary:

B_w of 10.50 km^3, B_s : -26.50 km^3 and B_n : -16.00 km^3 , AAR = 46%

Specific values:
b_w= 1.32 m, b_s= -3.33, b_n= -2.01 m

Appendix A: Mass balance at measurement sites 2009_10.

b_w: specific winter balance, **b_s**: specific summer balance, **b_n**: specific net balance, **l_a**: new snow in autumn (all in water equivalent).

Site	Position				Elevation	Date	Date	b_w	b_s	b_n	la
	Latitude		Longitude		(m a.s.l.)	in spring	in autumn	(mm)	(mm)	(mm)	(mm)
B09q	64	45,4582	16	5,2337	729	100506	101007	500	-5800	-5300	0
B08q	64	45,3988	16	5,8022	737	100506	101007	470	-6212	-5742	0
B10r	64	43,6845	16	6,7010	822	100506	101007	619	-5506	-4887	
B12p	64	38,2787	16	14,1600	1078	100506	101007	1179	-3609	-2430	15
B13p	64	34,5167	16	19,7870	1215	100505	101007	1410	-2710	-1300	30
B14r	64	31,6438	16	24,6953	1313	100505	101007	1820	-2238	-418	75
B15e	64	28,5036	16	29,9941	1397	100505	101007	1680	-2160	-480	150
B16r	64	23,6123	16	42,0794	1525	100505	101008	1597	-1677	-80	288
B17p	64	36,7331	16	28,8076	1214	100506	101007	1271	-2966	-1695	15
Br1e	64	5,5271	16	19,4848	139	100430	101013	-1899	-9504	-11403	0
Br2g	64	6,4228	16	22,5528	260	100430	101013	-1480	-7025	-8505	0
Br3m	64	8,6556	16	23,6631	421	100430	101013	-1130	-5850	-6980	0
Br7n	64	22,1435	16	16,9213	1248	100508	101012	1700	-2966	-1266	102
B07p	64	25,7942	16	17,4307	1358	100508	101007	1947	-1917	30	240
BB0o	64	22,7137	16	5,0566	1520	100508	101006	2680	-1426	1254	342
B19n	64	27,9300	15	55,1645	1430	100507	101006	2253	-1239	1014	348
B18n	64	31,5747	16	0,1416	1311	100506	101006	1968	-2124	-156	90
gb2c	64	34,0658	16	0,0144	1201	100506	101006	1670	-2648	-978	45
Budo	64	35,9887	15	59,9064	1136	100506	101006	1604	-2930	-1326	15
Bruo	64	40,9953	15	55,2178	793	100506	101006	426	-5925	-5499	0
D05m	64	42,7031	16	54,0252	1174	100508	101011	1294	-4255	-2961	0
D07m	64	38,2591	16	59,3083	1371	100509	101011	1384	-2478	-1094	72
D09m	64	31,8036	17	0,5640	1580	100509	101011	1768	-2158	-390	210
D12n	64	28,9896	17	0,1305	1648	100508	101008	1568	-1682	-114	141
E01o	64	41,5156	15	33,4077	695	100507	101007	233	-6191	-5958	0
E02o	64	39,1306	15	35,9769	958	100507	101007	1700	-4832	-3132	0
E03VIRp	64	36,6489	15	36,9029	1189	100507	101007	2060	-2726	-666	90
E04o	64	34,9441	15	37,0811	1288	100507	101007	2180	-2042	138	90
Hof01h	64	32,1508	15	35,5560	1126	100507	101007	2610	-2974	-364	90
Hosp1f	64	25,8524	15	28,6935	89	100430	100930	-1859	-9369	-11228	0
K01q	64	35,3471	17	52,7642	983	100509	101011	546	-6297	-5751	0
K02r	64	35,1628	17	50,9438	1113	100509	101011	516	-5232	-4716	0
K03r	64	34,2483	17	46,3879	1303	100509	101011	858	-4404	-3546	15
K04r	64	33,2091	17	42,2438	1495	100509	101011	1628	-3860	-2232	
K05r	64	33,4631	17	35,4723	1686	100509	101010	2170	-3628	-1458	150
K06q	64	38,3633	17	31,3889	1966	100608	101010	2640	-1254	1386	165
K07m	64	29,1071	17	42,0208	1540	100509	101011	2190	-3246	-1056	84
S01e	64	8,7340	17	49,6890	870	100511		276			
S02i	64	12,1521	17	49,0341	1016	100511		829			
S04j	64	16,1970	17	48,2589	1165	100510	101010	1289	-3707	-2418	
T01nm	64	19,4518	18	8,8032	744	100504		225			
T02nm	64	19,6109	18	3,9478	955	100504		838			
T03nm	64	20,2086	17	58,5980	1084	100504	101009	855	-5040	-4185	0
T04nm	64	21,3400	17	51,5160	1229	100504	101009	992	-3926	-2934	
T05nl	64	22,3100	17	42,9330	1349	100504	101009	1254	-3684	-2430	102
T06nm	64	24,2730	17	36,5917	1463	100504	101009	1430	-3581	-2151	
T07nk	64	25,3055	17	31,1676	1566	100504	101009	1878	-3348	-1470	
T08nm	64	26,3026	17	27,7982	1639	100504	101009	1840	-3394	-1554	189

HAABj	64	20,9674	17	24,1188	1729	100609	101010	2290	-2074	216	225
BORTHNb	64	25,1225	17	19,1474	1428	100510	101010	1275	-3483	-2208	261
BORae	64	24,9142	17	20,2306	1422	100606		1497			
G02g	64	26,8616	17	17,6874	1562	100608	101010	1789	-2569	-780	210
G03h	64	28,4418	17	16,3563	1655	100608	101010	1490	-1874	-384	249
G04o	64	30,0193	17	15,0214	1686	100608	101010	2086	-1390	696	300
Go1n	64	33,9982	17	24,9526	1760	100509	101010	2270	-2306	-36	219
Skf01a	64	18,0061	16	5,0077	1284	100508	101006	2910	-2262	648	165
Fl01a	64	25,9852	15	55,3520	1329	100507	101006	2710	-1876	834	150
Oer	63	59,7900	16	39,0400	1830	100430		4393		4393	

Appendix B: Balance distribution by elevation in 2009_10.

ΔS : area in elevation range, ∑ΔS: cumulative area above given elevation, b_w: specific winter balance, b_s: specific summer balance. b_n: specific winter balance, ΔB_w : winter balance at a given elevation range, $\sum\Delta B_w$: cumulative winter balance above given elevation, ΔB_s summer balance at a given elevation range, $\sum\Delta B_s$: cumulative summer balance above given elevation, ΔB_n: net annual balance in a given elevation range, $\sum B_n$: cumulative net annual balance above given elevation.

Vatnajökull

Elevation (m a.s.l.)			ΔS (km^2)	∑ΔS (km^2)	b_w (mm)	b_s (mm)	b_n (mm)	ΔB_w (10^6m^3)	$\sum\Delta B_w$ (10^6m^3)	ΔB_s (10^6m^3)	$\sum\Delta B_s$ (10^6m^3)	ΔB_n (10^6m^3)	$\sum B_n$ (10^6m^3)
2000	2050	2025	0,5	0,5	4110	-287	3823	2,0	2	-0,1	0	1,8	2
1950	2000	1975	16,3	16,8	2843	-1231	1611	46,4	48	-20,1	-20	26,3	28
1900	1950	1925	44,6	61,4	2718	-1337	1381	121,3	170	-59,7	-80	61,6	90
1850	1900	1875	35,8	97,2	2764	-1325	1438	98,9	269	-47,4	-127	51,5	141
1800	1850	1825	40,4	137,6	2795	-1191	1604	112,9	381	-48,1	-175	64,8	206
1750	1800	1775	55,5	193,1	2513	-1696	816	139,5	521	-94,2	-270	45,3	251
1700	1750	1725	102,5	295,6	2265	-2147	117	232,3	753	-220,2	-490	12,1	263
1650	1700	1675	223,9	519,5	1995	-2023	-27	447,0	1200	-453,2	-943	-6,2	257
1600	1650	1625	355,2	874,7	1850	-2030	-180	657,2	1857	-721,2	-1664	-64,0	193
1550	1600	1575	355,7	1230,4	1783	-2127	-343	634,6	2492	-756,9	-2421	-122,3	71
1500	1550	1525	418,4	1648,8	1726	-2217	-491	722,1	3214	-927,5	-3349	-205,4	-135
1450	1500	1475	450,3	2099,1	1719	-2328	-608	774,4	3988	-1048,5	-4397	-274,1	-409
1400	1450	1425	502,0	2601,1	1756	-2280	-523	882,0	4870	-1145,0	-5542	-263,1	-672
1350	1400	1375	537,1	3138,2	1802	-2289	-486	968,3	5839	-1229,8	-6772	-261,5	-933
1300	1350	1325	549,0	3687,2	1761	-2488	-726	967,2	6806	-1366,1	-8138	-398,8	-1332
1250	1300	1275	518,8	4206,0	1694	-2722	-1027	879,0	7685	-1412,2	-9550	-533,2	-1865
1200	1250	1225	463,8	4669,8	1555	-3061	-1505	721,6	8407	-1419,7	-10970	-698,2	-2563
1150	1200	1175	411,2	5081,0	1451	-3381	-1930	596,7	9003	-1390,4	-12360	-793,7	-3357
1100	1150	1125	367,9	5448,9	1369	-3695	-2325	503,9	9507	-1359,5	-13720	-855,6	-4213
1050	1100	1075	331,3	5780,2	1245	-4048	-2802	412,7	9920	-1341,1	-15061	-928,4	-5141
1000	1050	1025	306,2	6086,4	1121	-4369	-3247	343,6	10263	-1337,8	-16399	-994,3	-6135
950	1000	975	278,9	6365,3	967	-4600	-3633	269,7	10533	-1282,8	-17682	-1013,1	-7149
900	950	925	239,7	6605,0	807	-4780	-3972	193,5	10727	-1145,6	-18827	-952,1	-8101
850	900	875	216,1	6821,1	645	-4975	-4330	139,4	10866	-1075,0	-19902	-935,7	-9036
800	850	825	197,8	7018,9	491	-5198	-4707	97,1	10963	-1028,4	-20931	-931,2	-9968
750	800	775	170,7	7189,6	334	-5442	-5107	57,1	11020	-929,0	-21860	-871,9	-10839
700	750	725	135,1	7324,7	157	-5494	-5336	21,2	11041	-742,0	-22602	-720,8	-11560
650	700	675	101,6	7426,3	8	-5428	-5419	0,9	11042	-551,3	-23153	-550,4	-12111
600	650	625	70,3	7496,6	-195	-5297	-5493	-13,8	11029	-372,6	-23525	-386,4	-12497
550	600	575	63,4	7560,0	-394	-5288	-5682	-25,0	11004	-335,3	-23861	-360,3	-12857
500	550	525	44,7	7604,7	-584	-5439	-6024	-26,1	10977	-243,0	-24104	-269,1	-13126
450	500	475	41,4	7646,1	-838	-5613	-6451	-34,7	10943	-232,7	-24336	-267,4	-13394
400	450	425	44,4	7690,5	-995	-5794	-6790	-44,2	10898	-257,4	-24594	-301,6	-13695
350	400	375	40,6	7731,1	-1181	-5981	-7162	-48,0	10850	-242,9	-24837	-290,9	-13986
300	350	325	41,1	7772,2	-1326	-6343	-7669	-54,5	10796	-260,6	-25097	-315,1	-14301
250	300	275	40,4	7812,6	-1452	-6881	-8333	-58,7	10737	-278,0	-25375	-336,7	-14638
200	250	225	37,9	7850,5	-1572	-7635	-9208	-59,6	10678	-289,4	-25665	-349,0	-14987
150	200	175	31,6	7882,1	-1687	-8254	-9942	-53,3	10624	-260,5	-25925	-313,8	-15301
100	150	125	32,4	7914,5	-1813	-8800	-10614	-58,8	10566	-285,5	-26211	-344,3	-15645
50	100	75	24,7	7939,2	-1947	-9378	-11326	-48,1	10517	-231,8	-26443	-280,0	-15925
0	50	25	6,1	7945,3	-2007	-10105	-12113	-12,3	10505	-62,1	-26505	-74,4	-16000

Tungnaárjökull

Elevation (m a.s.l.)			ΔS (km^2)	$\sum\Delta S$ (km^2)	b_w (mm)	b_s (mm)	b_n (mm)	ΔB_w (10^6m^3)	$\sum\Delta B_w$ (10^6m^3)	ΔB_s (10^6m^3)	$\sum\Delta B_s$ (10^6m^3)	ΔB_n (10^6m^3)	$\sum B_n$ (10^6m^3)
1650	1700	1675	2,4	2,4	1953	-3300	-1346	4,6	5	-7,8	-8	-3,2	-3
1600	1650	1625	13,2	15,6	1970	-3425	-1455	25,9	31	-45,1	-53	-19,2	-22
1550	1600	1575	15,3	30,9	1967	-3486	-1518	30,0	61	-53,2	-106	-23,2	-46
1500	1550	1525	15,3	46,2	1797	-3532	-1734	27,5	88	-54,0	-160	-26,5	-72
1450	1500	1475	18,5	64,7	1541	-3584	-2042	28,5	117	-66,2	-226	-37,7	-110
1400	1450	1425	23,3	88,0	1363	-3633	-2269	31,8	148	-84,7	-311	-52,9	-163
1350	1400	1375	21,7	109,7	1274	-3672	-2398	27,6	176	-79,5	-391	-51,9	-215
1300	1350	1325	28,1	137,8	1170	-3723	-2552	32,8	209	-104,4	-495	-71,6	-286
1250	1300	1275	21,8	159,6	1082	-3803	-2721	23,6	232	-83,0	-578	-59,4	-346
1200	1250	1225	24,0	183,6	1003	-3974	-2971	24,1	257	-95,5	-674	-71,4	-417
1150	1200	1175	21,0	204,6	943	-4270	-3326	19,8	276	-89,5	-763	-69,7	-487
1100	1150	1125	19,2	223,8	896	-4662	-3765	17,2	294	-89,7	-853	-72,5	-559
1050	1100	1075	20,0	243,8	861	-5040	-4179	17,2	311	-100,8	-954	-83,5	-643
1000	1050	1025	18,2	262,0	823	-5313	-4490	15,0	326	-96,7	-1050	-81,7	-724
950	1000	975	18,9	280,9	751	-5571	-4819	14,2	340	-105,2	-1155	-91,0	-815
900	950	925	15,2	296,1	648	-5846	-5197	9,8	350	-88,7	-1244	-78,9	-894
850	900	875	15,1	311,2	530	-6127	-5597	8,0	358	-92,4	-1337	-84,4	-979
800	850	825	14,1	325,3	396	-6428	-6032	5,6	363	-90,5	-1427	-84,9	-1064
750	800	775	10,3	335,6	278	-6695	-6417	2,9	366	-68,7	-1496	-65,8	-1130
700	750	725	7,1	342,7	176	-7055	-6878	1,3	368	-50,4	-1546	-49,1	-1179
650	700	675	1,6	344,3	118	-7353	-7235	0,2	368	-12,1	-1558	-11,9	-1191
600	650	625	0,0	344,3	87	-7564	-7477	0,0	368	-0,5	-1559	-0,4	-1191

Sylgjujökull

Elevation (m a.s.l.)			ΔS (km^2)	$\sum\Delta S$ (km^2)	b_w (mm)	b_s (mm)	b_n (mm)	ΔB_w (10^6m^3)	$\sum\Delta B_w$ (10^6m^3)	ΔB_s (10^6m^3)	$\sum\Delta B_s$ (10^6m^3)	ΔB_n (10^6m^3)	$\sum B_n$ (10^6m^3)
1600	1650	1625	2,0	2,0	2175	-3515	-1339	4,4	4	-7,1	-7	-2,7	-3
1550	1600	1575	6,8	8,8	2148	-3502	-1353	14,5	19	-23,6	-31	-9,1	-12
1500	1550	1525	18,9	27,7	2014	-3404	-1390	38,0	57	-64,2	-95	-26,2	-38
1450	1500	1475	12,3	40,0	1642	-3546	-1903	20,1	77	-43,5	-138	-23,3	-61
1400	1450	1425	8,2	48,2	1392	-3659	-2266	11,4	88	-30,1	-169	-18,6	-80
1350	1400	1375	5,1	53,3	1276	-3688	-2411	6,5	95	-18,7	-187	-12,2	-92
1300	1350	1325	5,3	58,6	1149	-3762	-2612	6,1	101	-19,8	-207	-13,8	-106
1250	1300	1275	10,4	69,0	1056	-3886	-2829	10,9	112	-40,2	-247	-29,3	-135
1200	1250	1225	12,6	81,6	993	-4057	-3063	12,5	124	-51,0	-298	-38,5	-174
1150	1200	1175	14,4	96,0	951	-4279	-3328	13,7	138	-61,5	-360	-47,8	-222
1100	1150	1125	13,2	109,2	911	-4563	-3651	12,0	150	-60,2	-420	-48,1	-270
1050	1100	1075	13,4	122,6	828	-4915	-4087	11,1	161	-65,8	-486	-54,7	-325
1000	1050	1025	9,3	131,9	668	-5391	-4722	6,2	167	-49,9	-536	-43,7	-368
950	1000	975	3,1	135,0	622	-5541	-4918	1,9	169	-17,0	-553	-15,1	-383
900	950	925	1,6	136,6	517	-5989	-5471	0,8	170	-9,6	-562	-8,8	-392
850	900	875	0,2	136,8	394	-6394	-5999	0,0	170	-1,2	-563	-1,1	-393

Köldukvíslarjökull

Elevation (m a.s.l.)			ΔS (km^2)	∑ΔS (km^2)	b_w (mm)	b_s (mm)	b_n (mm)	ΔB_w ($10^6 m^3$)	$\sum\Delta B_w$ ($10^6 m^3$)	ΔB_s ($10^6 m^3$)	$\sum\Delta B_s$ ($10^6 m^3$)	ΔB_n ($10^6 m^3$)	$\sum B_n$ ($10^6 m^3$)
1950	2000	1975	3,6	3,6	2665	-1398	1266	9,6	10	-5,0	-5	4,5	5
1900	1950	1925	12,4	16,0	2606	-1694	911	32,3	42	-21,0	-26	11,3	16
1850	1900	1875	5,9	21,9	2493	-2244	248	14,6	57	-13,2	-39	1,5	17
1800	1850	1825	6,0	27,9	2404	-2573	-168	14,4	71	-15,4	-55	-1,0	16
1750	1800	1775	10,5	38,4	2323	-2817	-494	24,5	95	-29,7	-84	-5,2	11
1700	1750	1725	17,9	56,3	2239	-3318	-1079	40,0	135	-59,3	-144	-19,3	-8
1650	1700	1675	15,6	71,9	2120	-3596	-1476	33,0	168	-56,0	-200	-23,0	-31
1600	1650	1625	13,8	85,7	2005	-3664	-1659	27,7	196	-50,6	-250	-22,9	-54
1550	1600	1575	19,2	104,9	1910	-3692	-1782	36,7	233	-71,0	-321	-34,3	-88
1500	1550	1525	20,9	125,8	1850	-3610	-1759	38,7	271	-75,4	-397	-36,8	-125
1450	1500	1475	19,3	145,1	1675	-3763	-2087	32,4	304	-72,7	-469	-40,3	-166
1400	1450	1425	14,2	159,3	1430	-3946	-2516	20,4	324	-56,2	-525	-35,8	-201
1350	1400	1375	15,3	174,6	1197	-4105	-2908	18,3	342	-62,7	-588	-44,4	-246
1300	1350	1325	17,5	192,1	962	-4289	-3326	16,8	359	-75,0	-663	-58,2	-304
1250	1300	1275	18,0	210,1	770	-4499	-3729	13,8	373	-80,9	-744	-67,0	-371
1200	1250	1225	18,3	228,4	649	-4791	-4142	11,9	385	-87,6	-832	-75,7	-447
1150	1200	1175	16,4	244,8	582	-5123	-4540	9,6	395	-84,0	-916	-74,5	-521
1100	1150	1125	14,9	259,7	535	-5469	-4934	8,0	403	-81,7	-997	-73,7	-595
1050	1100	1075	13,1	272,8	481	-5819	-5338	6,3	409	-76,2	-1074	-69,9	-665
1000	1050	1025	11,1	283,9	427	-6122	-5695	4,7	414	-67,8	-1141	-63,1	-728
950	1000	975	10,5	294,4	376	-6378	-6002	3,9	418	-66,7	-1208	-62,8	-791
900	950	925	5,6	300,0	343	-6576	-6233	1,9	419	-36,9	-1245	-35,0	-826
850	900	875	0,5	300,5	287	-6745	-6457	0,2	420	-3,6	-1249	-3,5	-829

Dyngjujökull

Elevation (m a.s.l.)			ΔS (km^2)	∑ΔS (km^2)	b_w (mm)	b_s (mm)	b_n (mm)	ΔB_w ($10^6 m^3$)	$\sum\Delta B_w$ ($10^6 m^3$)	ΔB_s ($10^6 m^3$)	$\sum\Delta B_s$ ($10^6 m^3$)	ΔB_n ($10^6 m^3$)	$\sum B_n$ ($10^6 m^3$)
1950	2000	1975	7,4	7,4	2669	-1234	1435	19,8	20	-9,1	-9	10,6	11
1900	1950	1925	23,2	30,6	2621	-1223	1398	60,7	81	-28,3	-38	32,4	43
1850	1900	1875	15,9	46,5	2478	-1404	1074	39,5	120	-22,4	-60	17,1	60
1800	1850	1825	9,7	56,2	2301	-1422	878	22,4	143	-13,9	-74	8,6	69
1750	1800	1775	16,0	72,2	2244	-1585	658	35,9	178	-25,3	-99	10,5	79
1700	1750	1725	27,3	99,5	2135	-1587	547	58,2	237	-43,3	-142	14,9	94
1650	1700	1675	71,6	171,1	1948	-1540	408	139,5	376	-110,3	-253	29,2	123
1600	1650	1625	114,0	285,1	1850	-1768	82	211,0	587	-201,6	-454	9,4	133
1550	1600	1575	94,7	379,8	1789	-2084	-294	169,5	757	-197,5	-652	-27,9	105
1500	1550	1525	89,7	469,5	1693	-2214	-521	151,8	908	-198,5	-850	-46,7	58
1450	1500	1475	75,1	544,6	1580	-2303	-722	118,7	1027	-173,0	-1023	-54,3	4
1400	1450	1425	61,4	606,0	1488	-2375	-886	91,4	1118	-145,8	-1169	-54,4	-51
1350	1400	1375	49,4	655,4	1410	-2494	-1084	69,7	1188	-123,2	-1292	-53,6	-104
1300	1350	1325	37,9	693,3	1363	-2690	-1326	51,7	1240	-102,0	-1394	-50,3	-155
1250	1300	1275	41,3	734,6	1343	-3018	-1674	55,5	1295	-124,7	-1519	-69,2	-224
1200	1250	1225	48,8	783,4	1317	-3538	-2221	64,3	1360	-172,8	-1692	-108,5	-332
1150	1200	1175	48,2	831,6	1279	-4118	-2838	61,7	1421	-198,4	-1890	-136,8	-469
1100	1150	1125	44,0	875,6	1205	-4470	-3265	53,0	1474	-196,8	-2087	-143,7	-613
1050	1100	1075	33,1	908,7	1126	-4778	-3652	37,3	1512	-158,3	-2245	-121,0	-734
1000	1050	1025	35,5	944,2	1025	-5135	-4110	36,4	1548	-182,1	-2428	-145,7	-880
950	1000	975	30,8	975,0	884	-5499	-4615	27,2	1575	-169,2	-2597	-142,0	-1022
900	950	925	25,6	1000,6	698	-5837	-5138	17,9	1593	-149,5	-2746	-131,6	-1153
850	900	875	24,9	1025,5	508	-6154	-5645	12,7	1606	-153,3	-2900	-140,6	-1294
800	850	825	19,7	1045,2	366	-6447	-6080	7,2	1613	-127,3	-3027	-120,0	-1414
750	800	775	15,2	1060,4	280	-6801	-6520	4,2	1617	-103,1	-3130	-98,9	-1513
700	750	725	1,7	1062,1	254	-7022	-6768	0,4	1618	-12,2	-3142	-11,8	-1524

Brúarjökull

Elevation (m a.s.l.)			ΔS (km^2)	$\sum\Delta S$ (km^2)	b_w (mm)	b_s (mm)	b_n (mm)	ΔB_w (10^6m^3)	$\sum\Delta B_w$ (10^6m^3)	ΔB_s (10^6m^3)	$\sum\Delta B_s$ (10^6m^3)	ΔB_n (10^6m^3)	$\sum B_n$ (10^6m^3)
1850	1900	1875	0,8	0,8	1803	-960	843	1,5	2	-0,8	-1	0,7	1
1800	1850	1825	4,2	5,0	1831	-860	970	7,6	9	-3,6	-4	4,0	5
1750	1800	1775	3,0	8,0	1823	-1022	800	5,4	15	-3,0	-7	2,4	7
1700	1750	1725	3,7	11,7	1811	-1284	526	6,8	21	-4,8	-12	2,0	9
1650	1700	1675	5,3	17,0	1803	-1428	374	9,5	31	-7,5	-20	2,0	11
1600	1650	1625	44,4	61,4	1756	-1684	71	78,0	109	-74,9	-95	3,2	14
1550	1600	1575	47,6	109,0	1654	-1750	-96	78,8	188	-83,4	-178	-4,6	10
1500	1550	1525	69,8	178,8	1618	-1837	-219	113,1	301	-128,4	-306	-15,3	-6
1450	1500	1475	73,9	252,7	1646	-2019	-373	121,7	422	-149,3	-456	-27,6	-33
1400	1450	1425	108,1	360,8	1816	-1955	-138	196,4	619	-211,4	-667	-14,9	-48
1350	1400	1375	148,2	509,0	1889	-1949	-60	280,0	899	-288,9	-956	-8,9	-57
1300	1350	1325	151,3	660,3	1905	-2061	-155	288,4	1187	-312,0	-1268	-23,6	-81
1250	1300	1275	144,8	805,1	1792	-2300	-508	259,5	1447	-333,2	-1601	-73,6	-154
1200	1250	1225	121,8	926,9	1627	-2596	-969	198,2	1645	-316,3	-1917	-118,1	-272
1150	1200	1175	105,8	1032,7	1491	-2883	-1391	157,9	1803	-305,1	-2223	-147,2	-420
1100	1150	1125	86,8	1119,5	1378	-3204	-1825	119,6	1923	-278,1	-2501	-158,4	-578
1050	1100	1075	73,3	1192,8	1254	-3584	-2329	92,0	2015	-262,9	-2764	-170,9	-749
1000	1050	1025	65,6	1258,4	1104	-4010	-2905	72,5	2087	-263,2	-3027	-190,7	-940
950	1000	975	59,4	1317,8	959	-4438	-3478	57,0	2144	-263,4	-3290	-206,5	-1146
900	950	925	48,9	1366,7	831	-4806	-3975	40,7	2185	-235,1	-3525	-194,4	-1341
850	900	875	44,9	1411,6	724	-5124	-4400	32,5	2217	-229,9	-3755	-197,4	-1538
800	850	825	41,4	1453,0	621	-5431	-4809	25,7	2243	-224,7	-3980	-199,0	-1737
750	800	775	36,1	1489,1	520	-5746	-5225	18,8	2262	-207,4	-4187	-188,7	-1926
700	750	725	23,8	1512,9	415	-5989	-5574	9,9	2272	-142,3	-4330	-132,4	-2058
650	700	675	12,8	1525,7	316	-6114	-5798	4,0	2276	-78,1	-4408	-74,0	-2132
600	650	625	0,3	1526,0	257	-6181	-5924	0,0	2276	-2,0	-4410	-2,0	-2134

Eyjabakkajökull

Elevation (m a.s.l.)			ΔS (km^2)	$\sum\Delta S$ (km^2)	b_w (mm)	b_s (mm)	b_n (mm)	ΔB_w (10^6m^3)	$\sum\Delta B_w$ (10^6m^3)	ΔB_s (10^6m^3)	$\sum\Delta B_s$ (10^6m^3)	ΔB_n (10^6m^3)	$\sum B_n$ (10^6m^3)
1550	1600	1575	0,0	0,0	2799	-1354	1445	0,0	0	0,0	0	0,0	0
1500	1550	1525	0,0	0,0	2809	-1332	1477	0,3	0	-0,1	0	0,1	0
1450	1500	1475	1,0	1,0	2774	-1396	1377	2,7	3	-1,4	-2	1,3	2
1400	1450	1425	1,8	2,8	2744	-1447	1297	5,0	8	-2,7	-4	2,4	4
1350	1400	1375	2,5	5,3	2662	-1585	1077	6,7	15	-4,0	-8	2,7	7
1300	1350	1325	3,9	9,2	2558	-1708	850	10,0	25	-6,7	-15	3,3	10
1250	1300	1275	13,4	22,6	2307	-2107	199	30,8	56	-28,2	-43	2,7	13
1200	1250	1225	13,3	35,9	2206	-2442	-236	29,4	85	-32,5	-76	-3,1	9
1150	1200	1175	14,7	50,6	2062	-2809	-746	30,3	115	-41,3	-117	-11,0	-2
1100	1150	1125	12,3	62,9	1919	-3186	-1267	23,5	139	-39,1	-156	-15,5	-17
1050	1100	1075	10,6	73,5	1791	-3619	-1828	19,0	158	-38,3	-194	-19,4	-36
1000	1050	1025	10,1	83,6	1666	-4101	-2435	16,8	175	-41,4	-236	-24,6	-61
950	1000	975	7,7	91,3	1527	-4549	-3021	11,8	186	-35,2	-271	-23,4	-84
900	950	925	5,2	96,5	1348	-4856	-3508	6,9	193	-25,0	-296	-18,1	-102
850	900	875	3,9	100,4	1219	-5072	-3853	4,8	198	-19,8	-316	-15,0	-118
800	850	825	3,2	103,6	1086	-5287	-4200	3,4	202	-16,7	-332	-13,3	-131
750	800	775	3,4	107,0	840	-5505	-4665	2,8	204	-18,6	-351	-15,7	-147
700	750	725	3,3	110,3	493	-5831	-5338	1,6	206	-19,2	-370	-17,6	-164
650	700	675	1,7	112,0	284	-6121	-5837	0,5	207	-10,4	-381	-9,9	-174

Hoffellsjökull

Elevation (m a.s.l.)			ΔS (km^2)	$\sum\Delta S$ (km^2)	b_w (mm)	b_s (mm)	b_n (mm)	ΔB_w ($10^6 m^3$)	$\sum\Delta B_w$ ($10^6 m^3$)	ΔB_s ($10^6 m^3$)	$\sum\Delta B_s$ ($10^6 m^3$)	ΔB_n ($10^6 m^3$)	$\sum B_n$ ($10^6 m^3$)
1450	1500	1475	0,9	0,9	2776	-1391	1385	2,6	3	-1,3	-1	1,3	1
1400	1450	1425	6,7	7,6	2399	-1517	882	16,1	19	-10,2	-11	5,9	7
1350	1400	1375	10,0	17,6	2322	-1705	616	23,2	42	-17,0	-29	6,2	13
1300	1350	1325	15,4	33,0	2276	-1926	350	35,0	77	-29,6	-58	5,4	19
1250	1300	1275	33,6	66,6	2270	-2176	94	76,2	153	-73,0	-131	3,2	22
1200	1250	1225	26,8	93,4	2389	-2327	61	64,0	217	-62,3	-193	1,6	24
1150	1200	1175	18,2	111,6	2541	-2598	-56	46,2	263	-47,3	-241	-1,0	23
1100	1150	1125	17,5	129,1	2603	-2926	-322	45,5	309	-51,2	-292	-5,6	17
1050	1100	1075	13,6	142,7	2482	-3208	-726	33,7	342	-43,5	-335	-9,9	7
1000	1050	1025	10,0	152,7	2197	-3437	-1239	21,9	364	-34,3	-370	-12,4	-5
950	1000	975	9,0	161,7	1869	-3722	-1853	16,9	381	-33,6	-403	-16,7	-22
900	950	925	6,4	168,1	1568	-4110	-2541	10,1	391	-26,4	-430	-16,3	-38
850	900	875	4,3	172,4	1315	-4439	-3124	5,6	397	-19,0	-449	-13,3	-52
800	850	825	3,5	175,9	1201	-4670	-3468	4,2	401	-16,3	-465	-12,1	-64
750	800	775	3,8	179,7	1002	-4958	-3955	3,8	405	-18,7	-484	-15,0	-79
700	750	725	3,8	183,5	755	-5193	-4438	2,9	408	-19,7	-503	-16,8	-96
650	700	675	3,4	186,9	502	-5306	-4803	1,7	409	-17,8	-521	-16,1	-112
600	650	625	2,5	189,4	231	-5386	-5155	0,6	410	-13,3	-535	-12,7	-125
550	600	575	1,8	191,2	-42	-5476	-5518	0,0	410	-10,0	-545	-10,0	-135
500	550	525	1,5	192,7	-289	-5616	-5906	-0,4	410	-8,3	-553	-8,7	-143
450	500	475	0,9	193,6	-529	-5851	-6380	-0,5	409	-5,3	-558	-5,8	-149
400	450	425	0,9	194,5	-729	-6160	-6889	-0,7	408	-5,9	-564	-6,5	-156
350	400	375	0,6	195,1	-850	-6445	-7296	-0,5	408	-3,6	-568	-4,1	-160
300	350	325	0,9	196,0	-983	-6670	-7654	-0,9	407	-5,8	-573	-6,7	-166
250	300	275	2,1	198,1	-1183	-6998	-8181	-2,5	404	-15,0	-588	-17,5	-184
200	250	225	3,3	201,4	-1359	-7655	-9014	-4,4	400	-25,0	-613	-29,4	-213
150	200	175	2,6	204,0	-1536	-8248	-9785	-4,0	396	-21,4	-635	-25,4	-239
100	150	125	2,1	206,1	-1746	-8781	-10527	-3,7	392	-18,4	-653	-22,0	-261
50	100	75	2,8	208,9	-1992	-9435	-11428	-5,5	387	-26,2	-679	-31,8	-293
0	50	25	0,5	209,4	-2093	-9639	-11733	-1,1	386	-5,1	-685	-6,2	-299

Breiðamerkurjökull

Elevation (m a.s.l.)			ΔS (km^2)	∑ΔS (km^2)	b_w (mm)	b_s (mm)	b_n (mm)	ΔB_w ($10^6 m^3$)	$\sum\Delta B_w$ ($10^6 m^3$)	ΔB_s ($10^6 m^3$)	$\sum\Delta B_s$ ($10^6 m^3$)	ΔB_n ($10^6 m^3$)	$\sum B_n$ ($10^6 m^3$)
1900	1950	1925	0,0	0,0	4407	4	4412	0,2	0	0,0	0	0,2	0
1850	1900	1875	0,4	0,4	4384	-60	4323	1,6	2	0,0	0	1,6	2
1800	1850	1825	0,4	0,8	4307	-195	4112	1,9	4	0,0	0	1,9	4
1750	1800	1775	0,8	1,6	4158	-356	3801	3,4	7	-0,3	0	3,1	7
1700	1750	1725	2,5	4,1	3106	-648	2457	7,7	15	-1,6	-2	6,1	13
1650	1700	1675	5,8	9,9	2229	-893	1336	12,8	28	-5,1	-7	7,7	21
1600	1650	1625	15,8	25,7	1905	-1117	787	30,1	58	-17,7	-25	12,4	33
1550	1600	1575	25,7	51,4	1760	-1362	397	45,3	103	-35,0	-60	10,2	43
1500	1550	1525	32,2	83,6	1795	-1655	139	57,7	161	-53,3	-113	4,5	48
1450	1500	1475	44,3	127,9	1956	-1820	136	86,6	247	-80,6	-194	6,1	54
1400	1450	1425	58,3	186,2	1964	-1968	-3	114,6	362	-114,8	-309	-0,2	54
1350	1400	1375	88,7	274,9	1969	-2130	-161	174,6	537	-188,9	-498	-14,3	39
1300	1350	1325	96,9	371,8	1864	-2428	-563	180,8	717	-235,4	-733	-54,6	-16
1250	1300	1275	59,4	431,2	1746	-2773	-1026	103,8	821	-164,8	-898	-61,0	-77
1200	1250	1225	39,7	470,9	1624	-3015	-1390	64,5	886	-119,6	-1017	-55,2	-132
1150	1200	1175	32,6	503,5	1470	-3210	-1740	48,0	934	-104,8	-1122	-56,8	-189
1100	1150	1125	27,7	531,2	1287	-3413	-2125	35,7	969	-94,6	-1217	-58,9	-247
1050	1100	1075	24,1	555,3	1121	-3562	-2440	27,0	996	-85,7	-1302	-58,7	-306
1000	1050	1025	22,1	577,4	972	-3698	-2726	21,5	1018	-81,8	-1384	-60,3	-367
950	1000	975	24,5	601,9	793	-3876	-3083	19,4	1037	-95,0	-1479	-75,6	-442
900	950	925	27,3	629,2	676	-4030	-3353	18,5	1056	-110,1	-1589	-91,6	-534
850	900	875	26,2	655,4	526	-4204	-3677	13,8	1070	-110,0	-1699	-96,2	-630
800	850	825	26,0	681,4	356	-4401	-4045	9,3	1079	-114,6	-1814	-105,3	-735
750	800	775	25,3	706,7	160	-4605	-4445	4,0	1083	-116,3	-1930	-112,2	-848
700	750	725	23,9	730,6	9	-4770	-4760	0,2	1083	-114,1	-2044	-113,8	-961
650	700	675	30,8	761,4	-96	-4885	-4982	-3,0	1080	-150,7	-2195	-153,7	-1115
600	650	625	26,2	787,6	-313	-5120	-5434	-8,2	1072	-134,1	-2329	-142,3	-1257
550	600	575	26,8	814,4	-592	-5347	-5939	-15,9	1056	-143,5	-2473	-159,4	-1417
500	550	525	15,6	830,0	-739	-5465	-6204	-11,5	1044	-85,3	-2558	-96,8	-1513
450	500	475	16,2	846,2	-985	-5639	-6625	-16,0	1028	-91,5	-2649	-107,5	-1621
400	450	425	15,8	862,0	-1137	-5823	-6961	-17,9	1011	-91,7	-2741	-109,6	-1731
350	400	375	12,9	874,9	-1294	-6091	-7385	-16,6	994	-78,3	-2820	-95,0	-1826
300	350	325	12,9	887,8	-1428	-6508	-7937	-18,4	976	-84,0	-2903	-102,4	-1928
250	300	275	12,0	899,8	-1557	-7183	-8741	-18,7	957	-86,1	-2990	-104,8	-2033
200	250	225	11,5	911,3	-1691	-8183	-9874	-19,4	937	-93,9	-3083	-113,3	-2146
150	200	175	8,5	919,8	-1818	-9024	-10842	-15,5	922	-77,1	-3161	-92,6	-2239
100	150	125	7,9	927,7	-1915	-9577	-11492	-15,0	907	-75,2	-3236	-90,2	-2329
50	100	75	6,0	933,7	-1977	-9959	-11937	-11,9	895	-60,0	-3296	-71,9	-2401
0	50	25	2,9	936,6	-2001	-10158	-12160	-5,9	889	-29,9	-3326	-35,8	-2437

Síðujökull

Elevation (m a.s.l.)			ΔS (km^2)	∑ΔS (km^2)	b_w (mm)	b_s (mm)	b_n (mm)	$ΔB_w$ (10^6m^3)	$∑ΔB_w$ (10^6m^3)	$ΔB_s$ (10^6m^3)	$∑ΔB_s$ (10^6m^3)	$ΔB_n$ (10^6m^3)	$∑B_n$ (10^6m^3)
1700	1750	1725	0,7	0,7	2190	-2084	106	1,6	2	-1,6	-2	0,0	0
1650	1700	1675	5,2	5,9	2016	-2514	-497	10,4	12	-13,0	-15	-2,6	-3
1600	1650	1625	11,1	17,0	1939	-3011	-1071	21,6	34	-33,5	-48	-11,9	-14
1550	1600	1575	10,1	27,1	1921	-3018	-1096	19,4	53	-30,5	-79	-11,1	-26
1500	1550	1525	20,1	47,2	1858	-3128	-1269	37,4	91	-63,0	-142	-25,6	-51
1450	1500	1475	40,1	87,3	1721	-3274	-1553	69,0	160	-131,3	-273	-62,3	-113
1400	1450	1425	26,9	114,2	1535	-3485	-1950	41,3	201	-93,7	-367	-52,4	-166
1350	1400	1375	21,3	135,5	1468	-3530	-2062	31,3	232	-75,3	-442	-44,0	-210
1300	1350	1325	17,4	152,9	1432	-3556	-2123	25,0	257	-62,0	-504	-37,0	-247
1250	1300	1275	16,6	169,5	1365	-3632	-2266	22,6	280	-60,2	-564	-37,5	-284
1200	1250	1225	21,2	190,7	1345	-3623	-2278	28,5	308	-76,8	-641	-48,3	-333
1150	1200	1175	18,1	208,8	1270	-3715	-2444	23,0	331	-67,2	-708	-44,3	-377
1100	1150	1125	17,0	225,8	1129	-4310	-3180	19,2	350	-73,4	-781	-54,1	-431
1050	1100	1075	18,0	243,8	987	-4995	-4008	17,8	368	-89,9	-871	-72,1	-503
1000	1050	1025	21,8	265,6	857	-5539	-4681	18,7	387	-120,6	-992	-101,9	-605
950	1000	975	21,8	287,4	638	-5546	-4907	13,9	401	-121,0	-1113	-107,1	-712
900	950	925	22,1	309,5	449	-5395	-4946	10,0	411	-119,4	-1232	-109,4	-822
850	900	875	20,9	330,4	325	-5443	-5118	6,8	418	-113,6	-1346	-106,8	-928
800	850	825	25,0	355,4	189	-5485	-5296	4,7	422	-137,0	-1483	-132,3	-1061
750	800	775	25,5	380,9	31	-5707	-5675	0,8	423	-145,4	-1628	-144,6	-1205
700	750	725	26,0	406,9	-177	-6033	-6211	-4,6	418	-156,7	-1785	-161,3	-1367
650	700	675	15,8	422,7	-350	-6322	-6673	-5,6	413	-100,1	-1885	-105,6	-1472
600	650	625	7,4	430,1	-448	-6519	-6968	-3,3	410	-48,2	-1933	-51,6	-1524
550	600	575	0,2	430,3	-497	-6746	-7244	-0,1	409	-1,4	-1935	-1,5	-1525

Skaftárjökull

Elevation (m a.s.l.)			ΔS (km^2)	∑ΔS (km^2)	b_w (mm)	b_s (mm)	b_n (mm)	$ΔB_w$ (10^6m^3)	$∑ΔB_w$ (10^6m^3)	$ΔB_s$ (10^6m^3)	$∑ΔB_s$ (10^6m^3)	$ΔB_n$ (10^6m^3)	$∑B_n$ (10^6m^3)
1350	1400	1375	2,4	2,4	1309	-3657	-2348	3,2	3	-8,9	-9	-5,7	-6
1300	1350	1325	5,5	7,9	1257	-3697	-2439	6,9	10	-20,2	-29	-13,3	-19
1250	1300	1275	4,5	12,4	1200	-3735	-2535	5,4	15	-16,8	-46	-11,4	-30
1200	1250	1225	6,5	18,9	1149	-3788	-2638	7,4	23	-24,5	-70	-17,0	-48
1150	1200	1175	9,3	28,2	1073	-4010	-2937	9,9	33	-37,1	-108	-27,2	-75
1100	1150	1125	12,3	40,5	981	-4494	-3513	12,0	45	-55,1	-163	-43,0	-118
1050	1100	1075	14,2	54,7	913	-5143	-4230	12,9	58	-72,9	-235	-59,9	-178
1000	1050	1025	12,1	66,8	829	-5401	-4571	10,0	68	-65,4	-301	-55,3	-233
950	1000	975	7,6	74,4	668	-5380	-4711	5,1	73	-40,9	-342	-35,8	-269
900	950	925	5,3	79,7	506	-5499	-4992	2,7	76	-29,3	-371	-26,6	-295
850	900	875	5,6	85,3	351	-5803	-5452	1,9	78	-32,2	-403	-30,3	-326
800	850	825	5,7	91,0	206	-6203	-5997	1,2	79	-35,4	-439	-34,2	-360
750	800	775	5,1	96,1	90	-6490	-6399	0,5	79	-33,3	-472	-32,8	-393
700	750	725	3,6	99,7	-88	-6775	-6864	-0,3	79	-24,1	-496	-24,4	-417
650	700	675	2,8	102,5	-279	-6965	-7245	-0,8	78	-19,6	-516	-20,4	-438
600	650	625	0,8	103,3	-431	-7078	-7510	-0,3	78	-5,5	-521	-5,8	-443

Vestari Skaftárketill

Elevation (m a.s.l.)			ΔS (km^2)	$\sum \Delta S$ (km^2)	b_w (mm)	b_s (mm)	b_n (mm)	ΔB_w ($10^6 m^3$)	$\sum \Delta B_w$ ($10^6 m^3$)	ΔB_s ($10^6 m^3$)	$\sum \Delta B_s$ ($10^6 m^3$)	ΔB_n ($10^6 m^3$)	$\sum B_n$ ($10^6 m^3$)
1900	1950	1925	0,7	0,7	2569	-1702	867	1,7	2	-1,2	-1	0,6	1
1850	1900	1875	0,6	1,3	2515	-1892	622	1,5	3	-1,1	-2	0,4	1
1800	1850	1825	0,7	2,0	2443	-2184	258	1,8	5	-1,6	-4	0,2	1
1750	1800	1775	2,7	4,7	2309	-2632	-322	6,2	11	-7,1	-11	-0,9	0
1700	1750	1725	5,9	10,6	2243	-3209	-966	13,2	24	-18,8	-30	-5,7	-5
1650	1700	1675	6,7	17,3	2197	-3512	-1315	14,6	39	-23,4	-53	-8,7	-14
1600	1650	1625	7,4	24,7	2177	-3532	-1355	16,2	55	-26,2	-79	-10,1	-24
1550	1600	1575	5,2	29,9	2156	-3513	-1356	11,1	66	-18,1	-98	-7,0	-31
1500	1550	1525	1,5	31,4	2158	-3494	-1335	3,2	70	-5,1	-103	-2,0	-33

Eystri Skaftárketill

Elevation (m a.s.l.)			ΔS (km^2)	$\sum \Delta S$ (km^2)	b_w (mm)	b_s (mm)	b_n (mm)	ΔB_w ($10^6 m^3$)	$\sum \Delta B_w$ ($10^6 m^3$)	ΔB_s ($10^6 m^3$)	$\sum \Delta B_s$ ($10^6 m^3$)	ΔB_n ($10^6 m^3$)	$\sum B_n$ ($10^6 m^3$)
1750	1800	1775	1,1	1,1	2274	-2595	-320	2,5	3	-2,9	-3	-0,4	0
1700	1750	1725	11,1	12,2	2189	-2966	-777	24,4	27	-33,0	-36	-8,7	-9
1650	1700	1675	16,2	28,4	2105	-3139	-1034	34,1	61	-50,8	-87	-16,7	-26
1600	1650	1625	9,2	37,6	2131	-3405	-1273	19,7	81	-31,5	-118	-11,8	-38
1550	1600	1575	2,2	39,8	2137	-3446	-1308	4,7	85	-7,6	-126	-2,9	-40

Gjálp

Elevation (m a.s.l.)			ΔS (km^2)	$\sum \Delta S$ (km^2)	b_w (mm)	b_s (mm)	b_n (mm)	ΔB_w ($10^6 m^3$)	$\sum \Delta B_w$ ($10^6 m^3$)	ΔB_s ($10^6 m^3$)	$\sum \Delta B_s$ ($10^6 m^3$)	ΔB_n ($10^6 m^3$)	$\sum B_n$ ($10^6 m^3$)
1900	1950	1925	0,5	0,5	2578	-1580	997	1,4	1	-0,9	-1	0,5	1
1850	1900	1875	0,6	1,1	2495	-1805	690	1,5	3	-1,1	-2	0,4	1
1800	1850	1825	1,2	2,3	2397	-2104	292	2,8	6	-2,5	-5	0,3	1
1750	1800	1775	4,5	6,8	2283	-2370	-86	10,4	16	-10,8	-15	-0,4	1
1700	1750	1725	15,9	22,7	2147	-2298	-150	34,2	50	-36,6	-52	-2,4	-2
1650	1700	1675	16,5	39,2	2055	-2031	24	34,0	84	-33,6	-85	0,4	-1
1600	1650	1625	0,0	39,2	2049	-2056	-6	0,0	84	0,0	-85	0,0	-1

Grímsvötn

Elevation (m a.s.l.)			ΔS (km^2)	$\sum \Delta S$ (km^2)	b_w (mm)	b_s (mm)	b_n (mm)	ΔB_w ($10^6 m^3$)	$\sum \Delta B_w$ ($10^6 m^3$)	ΔB_s ($10^6 m^3$)	$\sum \Delta B_s$ ($10^6 m^3$)	ΔB_n ($10^6 m^3$)	$\sum B_n$ ($10^6 m^3$)
1700	1750	1725	0,8	0,8	1994	-1703	291	1,6	2	-1,4	-1	0,2	0
1650	1700	1675	40,8	41,6	1842	-2092	-249	75,2	77	-85,4	-87	-10,2	-10
1600	1650	1625	30,6	72,2	1742	-2628	-886	53,4	130	-80,5	-167	-27,2	-37
1550	1600	1575	18,6	90,8	1645	-2699	-1054	30,7	161	-50,3	-218	-19,6	-57
1500	1550	1525	16,9	107,7	1593	-2940	-1347	26,9	188	-49,6	-267	-22,7	-80
1450	1500	1475	11,6	119,3	1566	-3315	-1749	18,1	206	-38,4	-306	-20,3	-100
1400	1450	1425	15,1	134,4	1510	-3500	-1990	22,8	229	-52,7	-358	-30,0	-130
1350	1400	1375	0,6	135,0	1702	-3441	-1738	1,1	230	-2,2	-361	-1,1	-131

Appendix C: Coordinates at velocity measurement stakes.

Position of velocity measurement stakes determined by GPS sub-metre differential (I), fast static (FS) and kinematic (K).
(Accuracy of horizontal position 0.5 – 1.0 m, and vertical accuracy 1-2 m for DGPS, about 1cm for fast static, and 3 cm for kinematic).
The station Hofn in Höfn í Hornafirði is used as a stationary reference for all measurements, ÍSN93 datum, h_l is elevation above ellipsoid, dL antenna height, N estimated difference between ellipsoid and sea-level, H elevation in metres above sea level ($H= h_l+N+dL$). X and Y are ÍSN93 Lambert conformal conic projected coordinates. M is a quality marker.

Site	time	Date	#	Calender Day	Year	Latitude		Longitude		h_l (m a. e.)	dL (m)	N (m)	H (m a. s. l.)	X	Y	M
B07p	15,596	8	5	128	2010	64	25,79423	16	17,43072	1424,8	0,0	-67,1	1357,7	630494,60	439242,25	K
B07p	14,692	7	10	280	2010	64	25,79367	16	17,42988	1419,6	0,0	-67,1	1352,6	630495,31	439241,25	K
B08q	14,534	6	5	126	2010	64	45,39882	16	5,80222	803,7	0,0	-66,7	737,1	638150,19	476043,51	K
B08q	19,650	7	10	280	2010	64	45,39896	16	5,80208	796,6	0,0	-66,7	729,9	638150,29	476043,78	K
B09q	14,975	6	5	126	2010	64	45,45823	16	5,23369	795,7	0,0	-66,7	729,1	638595,67	476174,51	K
B09q	20,029	7	10	280	2010	64	45,45854	16	5,23379	789,0	0,0	-66,7	722,4	638595,56	476175,10	K
B10r	13,738	6	5	126	2010	64	43,68449	16	6,70096	888,5	0,0	-66,7	821,7	637583,41	472828,96	K
B10r	21,142	7	10	280	2010	64	43,68503	16	6,70128	882,0	0,0	-66,7	815,3	637583,10	472829,94	K
B12p	10,671	6	5	126	2010	64	38,27873	16	14,16003	1145,1	0,0	-66,9	1078,2	632104,46	462529,91	K
B12p	23,179	7	10	280	2010	64	38,28858	16	14,15072	1141,8	0,0	-66,9	1074,9	632111,07	462548,52	K
B13p	19,596	5	5	125	2010	64	34,51674	16	19,78702	1281,9	0,0	-67,0	1214,9	627919,99	455353,72	K
B13p	16,404	7	10	280	2010	64	34,52798	16	19,77456	1276,8	0,0	-67,0	1209,8	627929,05	455375,01	K
B14p	15,650	7	10	280	2010	64	31,67797	16	24,62422	1374,9	0,0	-67,1	1307,8	624275,98	449923,05	K
B14r	16,979	5	5	125	2010	64	31,64381	16	24,69527	1380,5	0,0	-67,1	1313,4	624221,78	449857,30	K
B14r	12,071	8	10	281	2010	64	31,65190	16	24,68289	1375,2	0,0	-67,1	1308,1	624231,06	449872,73	K
B15e	16,129	5	5	125	2010	64	28,50362	16	29,99408	1463,9	0,0	-67,2	1396,7	620216,41	443856,83	K
B15e	15,321	7	10	280	2010	64	28,50851	16	29,98173	1458,7	0,0	-67,2	1391,5	620225,95	443866,30	K
B16r	14,942	5	5	125	2010	64	23,61228	16	42,07935	1592,7	0,0	-67,3	1525,3	610865,98	434407,12	K
B16r	12,713	8	10	281	2010	64	23,61014	16	42,08276	1587,5	0,0	-67,3	1520,2	610863,38	434403,05	K
B17p	9,221	6	5	126	2010	64	36,73308	16	28,80760	1280,9	0,0	-67,1	1213,8	620557,45	459172,73	K
B17p	16,063	7	10	280	2010	64	36,74045	16	28,80286	1276,5	0,0	-67,1	1209,4	620560,68	459186,57	K
B18m	16,096	6	10	279	2010	64	31,58806	16	0,14148	1373,5	0,0	-66,9	1306,6	643852,52	450621,51	K
B18n	18,596	6	5	126	2010	64	31,57470	16	0,14156	1378,3	0,0	-66,9	1311,4	643853,64	450596,70	K
B19n	19,284	7	5	127	2010	64	27,93004	15	55,16448	1496,8	0,0	-66,9	1429,9	648161,14	444024,35	K
B19n	15,009	6	10	279	2010	64	27,92953	15	55,16312	1491,2	0,0	-66,9	1424,3	648162,27	444023,45	K
BB0o	11,534	8	5	128	2010	64	22,71372	16	5,05656	1587,1	0,0	-66,9	1520,2	640684,44	433966,67	K
BB0o	14,021	6	10	279	2010	64	22,71358	16	5,05717	1581,8	0,0	-66,9	1515,0	640683,97	433966,38	K
BORae	18,763	6	6	157	2010	64	24,91421	17	20,23055	1489,3	0,0	-67,7	1421,6	580143,37	435864,34	K
BORTHNb	8,600	14	3	73	2010	64	25,12456	17	19,14707	1494,8	0,0	-67,7	1427,1	581003,12	436278,04	FS
BORTHNb	11,317	10	5	130	2010	64	25,12247	17	19,14740	1495,2	0,0	-67,7	1427,5	581002,96	436274,16	K
BORTHNb	20,821	6	6	157	2010	64	25,12142	17	19,14537	1496,0	-3,2	-67,7	1425,1	581004,64	436272,24	K
BORTHNb	17,325	10	10	283	2010	64	25,11278	17	19,14708	1523,6	-5,9	-67,7	1450,0	581003,69	436256,17	K
Br1d	12,450	30	1	30	2010	64	5,52782	16	19,48328	204,5	0,0	-65,8	138,7	630441,05	401550,40	FS
Br1e	12,989	30	1	30	2010	64	5,52714	16	19,48476	204,8	0,0	-65,8	139,0	630439,90	401549,08	FS
Br1e	15,450	23	8	235	2010	64	5,52471	16	19,48460	196,0	0,0	-65,8	130,2	630440,23	401544,56	K
Br1e	11,913	13	10	286	2010	64	5,52432	16	19,48445	194,2	0,0	-65,8	128,3	630439,59	401543,70	K
Br1f	11,913	13	10	286	2010	64	5,52407	16	19,48495	194,2	0,0	-65,8	128,3	630439,99	401543,37	K
Br2f	14,266	30	1	30	2010	64	6,42382	16	22,54593	326,7	0,0	-66,0	260,7	627884,60	403109,45	FS
Br2g	14,632	30	1	30	2010	64	6,42280	16	22,55280	325,9	0,0	-66,0	259,8	627879,10	403107,32	FS
Br2g	16,671	13	10	286	2010	64	6,41780	16	22,55278	318,1	0,0	-66,0	252,1	627879,52	403098,10	K
Br2h	16,671	13	10	286	2010	64	6,41780	16	22,55116	318,1	0,0	-66,0	252,1	627880,82	403098,10	K
Br3l	16,530	30	1	30	2010	64	8,67817	16	23,68738	488,5	0,0	-66,3	422,2	626785,47	407256,23	FS
Br3m	16,253	30	1	30	2010	64	8,65557	16	23,66313	487,6	0,0	-66,3	421,3	626806,86	407215,08	FS
Br3m	15,184	13	10	286	2010	64	8,64238	16	23,65215	481,8	0,0	-66,3	415,5	626816,77	407190,97	K
Br3n	15,000	13	10	286	2010	64	8,54946	16	24,16552	481,3	0,0	-66,3	415,0	626407,68	407001,32	K
Br7n	14,900	8	5	128	2010	64	22,14352	16	16,92132	1315,2	0,0	-67,0	1248,2	631194,78	432483,06	K
Br7n	13,084	12	10	285	2010	64	22,12088	16	16,91694	1309,2	0,0	-67,0	1242,2	631200,11	432441,19	FS

BreSp01	14,146	23	8	235	2010	64	5,16192	16	19,73733	123,1	0,0	-65,8	57,3	630263,44	400862,41	K
BrPu01a	14,234	23	8	235	2010	64	5,23978	16	19,74652	142,2	0,0	-65,8	76,3	630249,86	401006,63	K
BrPu02a	14,354	23	8	235	2010	64	5,36992	16	19,75695	169,6	0,0	-65,8	103,7	630231,18	401247,87	K
BrPu03a	14,471	23	8	235	2010	64	5,50207	16	19,70012	195,0	0,0	-65,9	129,1	630266,97	401495,13	K
Bruo	16,092	6	5	126	2010	64	40,99525	15	55,21775	860,0	0,0	-66,7	793,2	646936,34	468268,59	K
Bruo	18,987	6	10	279	2010	64	40,99612	15	55,21828	850,3	0,0	-66,7	783,6	646935,84	468270,17	K
Budo	16,904	6	5	126	2010	64	35,98870	15	59,90642	1202,8	0,0	-66,9	1136,0	643652,32	458797,58	K
Budo	18,084	6	10	279	2010	64	36,00044	15	59,90496	1197,7	0,0	-66,9	1130,8	643652,45	458819,42	K
D05m	20,154	8	5	128	2010	64	42,70312	16	54,02518	1241,6	0,0	-67,3	1174,3	600089,32	469524,24	K
D05m	12,096	11	10	284	2010	64	42,70855	16	54,01554	1237,9	0,0	-67,3	1170,6	600096,63	469534,58	K
D07h	11,246	11	10	284	2010	64	38,40431	16	59,15951	1423,7	0,0	-67,5	1356,2	596265,82	461408,39	K
D07k	11,184	11	10	284	2010	64	38,34955	16	59,20273	1428,1	0,0	-67,5	1360,6	596234,64	461305,59	K
D07m	11,538	9	5	129	2010	64	38,25913	16	59,30826	1438,3	0,0	-67,5	1370,8	596155,94	461135,01	K
D07m	10,767	11	10	284	2010	64	38,27162	16	59,29622	1433,3	0,0	-67,5	1365,8	596164,79	461158,50	K
D09l	10,071	11	10	284	2010	64	31,81454	17	0,57364	1642,8	0,0	-67,6	1575,2	595525,09	449135,01	K
D09m	12,292	9	5	129	2010	64	31,80358	17	0,56399	1647,8	0,0	-67,6	1580,2	595533,45	449114,90	K
D09m	10,317	11	10	284	2010	64	31,80759	17	0,56541	1642,6	0,0	-67,6	1575,1	595532,08	449122,31	K
D12n	17,438	8	5	128	2010	64	28,98963	17	0,13052	1715,6	0,0	-67,6	1648,0	596045,25	443900,14	K
D12n	15,329	8	10	281	2010	64	28,99001	17	0,13065	1710,4	0,0	-67,6	1642,9	596045,13	443900,84	K
E01o	15,800	7	5	127	2010	64	41,51556	15	33,40766	762,0	0,0	-66,7	695,3	664210,55	470128,59	K
E01o	10,784	7	10	280	2010	64	41,51574	15	33,40755	755,4	0,0	-66,7	688,7	664210,63	470128,93	K
E02o	14,384	7	5	127	2010	64	39,13055	15	35,97692	1024,9	0,0	-66,8	958,1	662408,59	465593,12	K
E02o	10,238	7	10	280	2010	64	39,14026	15	35,97253	1017,7	0,0	-66,8	950,9	662411,12	465611,32	K
E03o	9,879	7	10	280	2010	64	36,66461	15	36,92262	1248,8	0,0	-66,9	1181,9	661901,70	460977,58	K
E03STlKp	13,959	7	5	127	2010	64	36,64948	15	36,90897	1255,2	0,0	-66,9	1188,4	661914,08	460950,08	K
E03STlKp	9,792	7	10	280	2010	64	36,65452	15	36,91285	1249,4	0,0	-66,9	1182,6	661910,48	460959,28	K
E03VIRp	13,746	7	5	127	2010	64	36,64894	15	36,90291	1255,4	0,0	-66,9	1188,6	661918,96	460949,35	K
E03VIRp	9,721	7	10	280	2010	64	36,65365	15	36,90482	1249,4	0,0	-66,9	1182,6	661916,97	460957,99	K
E04o	10,284	7	5	127	2010	64	34,94413	15	37,08106	1355,2	0,0	-66,8	1288,3	661946,43	457778,74	K
E04o	9,092	7	10	280	2010	64	34,94468	15	37,08037	1350,4	0,0	-66,8	1283,5	661946,93	457779,78	K
Fl01a	19,075	7	5	127	2010	64	25,98516	15	55,35204	1396,2	0,0	-66,8	1329,4	648186,76	440407,71	K
Fl01a	15,529	6	10	279	2010	64	25,97783	15	55,33501	1389,8	0,0	-66,8	1323,0	648201,08	440394,78	K
G02g	23,513	8	6	159	2010	64	26,86164	17	17,68739	1629,6	0,0	-67,7	1561,9	582088,17	439535,77	K
G02g	16,092	10	10	283	2010	64	26,85853	17	17,68996	1624,5	0,0	-67,7	1556,8	582086,27	439529,94	K
G03h	22,349	8	6	159	2010	64	28,44181	17	16,35633	1722,8	0,0	-67,7	1655,1	583075,64	442499,62	K
G03h	15,788	10	10	283	2010	64	28,43166	17	16,35999	1718,5	0,0	-67,7	1650,8	583073,23	442480,67	K
G04o	14,138	8	6	159	2010	64	30,01925	17	15,02135	1753,4	0,0	-67,7	1685,7	584064,32	445458,79	K
G04o	10,184	10	10	283	2010	64	30,01144	17	15,02233	1749,5	0,0	-67,7	1681,8	584063,94	445444,26	K
gb2rora	17,534	6	5	126	2010	64	34,06577	16	0,01438	1268,7	0,0	-66,9	1201,8	643735,74	455224,71	K
gb2rorb	16,846	6	10	279	2010	64	34,07347	16	0,01627	1267,7	0,0	-66,9	1200,8	643733,55	455238,94	K
gb2c	17,534	6	5	126	2010	64	34,06577	16	0,01438	1268,7	-0,9	-66,9	1200,9	643735,74	455224,71	K
gb2c	16,846	6	10	279	2010	64	34,07347	16	0,01627	1267,7	-6,0	-66,9	1194,8	643733,55	455238,94	K
Go1m	11,213	10	10	283	2010	64	33,99754	17	24,94753	1821,6	0,0	-67,8	1753,8	575932,22	452638,53	K
Go1n	13,492	9	5	129	2010	64	33,99819	17	24,95256	1827,9	0,0	-67,8	1760,0	575928,17	452639,62	K
Go1n	11,038	10	10	283	2010	64	33,99597	17	24,95266	1822,2	0,0	-67,8	1754,3	575928,19	452635,51	K
HAABj	15,863	9	6	160	2010	64	20,96739	17	24,11877	1796,4	0,0	-67,5	1728,8	577206,05	428452,91	K
HAABj	16,284	10	10	283	2010	64	20,96769	17	24,11901	1791,0	0,0	-67,5	1723,5	577205,84	428453,46	K
Hof01h	13,067	7	5	127	2010	64	32,15077	15	35,55601	1192,4	0,0	-66,7	1125,7	663441,99	452661,58	K
Hof01h	10,334	7	10	280	2010	64	32,14316	15	35,55390	1185,8	0,0	-66,7	1119,1	663444,44	452647,56	K
Hosp1e	12,536	29	1	29	2010	64	25,85450	15	28,69822	154,9	0,0	-65,8	89,1	669570,21	441281,74	FS
Hosp1f	13,368	29	1	29	2010	64	25,85239	15	28,69350	154,7	0,0	-65,8	88,8	669574,21	441278,03	FS
Hosp1f	10,759	24	8	236	2010	64	25,84456	15	28,68798	145,9	0,0	-65,8	80,1	669579,44	441263,75	K
SvinAurA	11,167	24	8	236	2010	64	25,64735	15	28,71285	89,3	0,0	-65,8	23,5	669579,90	440896,79	K
HoUtfal1	12,034	24	8	236	2010	64	25,77660	15	27,47692	107,3	0,0	-65,8	41,5	670557,38	441191,99	K
HoUtfal2	12,050	24	8	236	2010	64	25,77432	15	27,47428	98,1	0,0	-65,8	32,4	670559,74	441187,87	K
K01q	18,063	9	5	129	2010	64	35,34710	17	52,76415	1050,4	0,0	-67,6	982,8	553669,40	454670,21	K
K01q	11,217	11	10	284	2010	64	35,34778	17	52,76650	1043,9	0,0	-67,6	976,3	553667,50	454671,44	K
K02r	17,509	9	5	129	2010	64	35,16283	17	50,94375	1180,7	0,0	-67,6	1113,1	555128,57	454354,01	K
K02r	10,921	11	10	284	2010	64	35,16557	17	50,95464	1175,1	0,0	-67,6	1107,5	555119,78	454358,93	K
K04r	19,004	9	5	129	2010	64	33,20911	17	42,24380	1562,3	0,0	-67,7	1494,5	562147,35	450859,17	K
K04r	11,788	11	10	284	2010	64	33,21301	17	42,26953	1554,7	0,0	-67,7	1487,0	562126,64	450865,99	K
K05q	13,292	10	10	283	2010	64	33,45119	17	35,51609	1744,6	0,0	-67,8	1676,8	567513,66	451423,85	K
K05r	14,484	9	5	129	2010	64	33,46310	17	35,47225	1753,5	0,0	-67,8	1685,6	567548,20	451446,75	K
K05r	13,809	10	10	283	2010	64	33,45965	17	35,48902	1745,4	0,0	-67,8	1677,6	567534,95	451440,03	K

K06q	18,492	8	6	159	2010	64	38,36326	17	31,38887	2033,6	0,0	-67,9	1965,7	570598,07	460623,22	K
K06q	11,800	10	10	283	2010	64	38,36131	17	31,39003	2036,0	-2,5	-67,9	1968,1	570597,24	460619,57	K
K07m	15,859	9	5	129	2010	64	29,10714	17	42,02076	1607,9	0,0	-67,7	1540,2	562482,27	443243,01	K
K07m	9,950	11	10	284	2010	64	29,10685	17	42,02877	1600,7	0,0	-67,7	1533,0	562475,86	443242,33	K
S02i	9,588	11	5	131	2010	64	12,15210	17	49,03413	1082,8	0,0	-67,0	1015,8	557452,74	411635,56	K
S04j	18,504	10	5	130	2010	64	16,19699	17	48,25886	1232,0	0,0	-67,2	1164,8	557938,17	419161,53	K
S04j	14,609	10	10	283	2010	64	16,18570	17	48,27040	1225,9	0,0	-67,2	1158,7	557929,24	419140,38	K
Skf01a	13,404	8	5	128	2010	64	18,00614	16	5,00771	1350,2	0,0	-66,6	1283,6	641127,09	425231,06	K
Skf01a	13,100	6	10	279	2010	64	18,00353	16	4,99217	1344,4	0,0	-66,6	1277,7	641139,84	425226,80	K
T01nm	9,313	4	5	124	2010	64	19,45183	18	8,80324	811,4	0,0	-67,3	744,2	541266,10	424939,62	K
T02nm	9,967	4	5	124	2010	64	19,61091	18	3,94784	1021,8	0,0	-67,3	954,5	545175,06	425290,49	K
T03nm	13,025	4	5	124	2010	64	20,20858	17	58,59796	1151,5	0,0	-67,3	1084,2	549468,44	426467,57	K
T03nm	17,996	9	10	282	2010	64	20,20622	17	58,61179	1145,0	0,0	-67,3	1077,7	549457,37	426463,01	K
T04nm	14,013	4	5	124	2010	64	21,34004	17	51,51597	1296,2	0,0	-67,4	1228,8	555135,49	428667,19	K
T04nm	15,038	5	6	156	2010	64	21,33936	17	51,51901	1294,5	0,0	-67,4	1227,1	555133,07	428665,89	K
T04nm	16,042	9	10	282	2010	64	21,33635	17	51,52994	1288,7	0,0	-67,4	1221,4	555124,37	428660,13	K
T05nl	12,750	13	3	72	2010	64	22,31067	17	42,93125	1417,3	-2,1	-67,5	1347,7	562009,39	430602,87	FS
T05nl	14,254	4	5	124	2010	64	22,31001	17	42,93302	1417,8	-1,8	-67,5	1348,6	562007,98	430601,60	K
T05nl	14,871	9	10	282	2010	64	22,30617	17	42,94249	1412,9	-4,3	-67,5	1341,2	562000,51	430594,32	K
T05rord	12,750	13	3	72	2010	64	22,31067	17	42,93125	1417,3	0,0	-67,5	1349,8	562009,39	430602,87	FS
T05rord	14,254	4	5	124	2010	64	22,31001	17	42,93302	1417,8	0,0	-67,5	1350,3	562007,98	430601,60	K
T05rord	16,871	5	6	156	2010	64	22,30958	17	42,93539	1417,7	0,0	-67,5	1350,2	562006,09	430600,76	K
T05rord	13,134	11	6	162	2010	64	22,30832	17	42,93402	1413,0	3,0	-67,5	1348,5	562007,25	430598,45	K
T05rore	13,134	11	6	162	2010	64	22,30832	17	42,93402	1413,0	0,0	-67,5	1345,5	562007,25	430598,45	K
T05rore	14,871	9	10	282	2010	64	22,30617	17	42,94249	1412,9	0,7	-67,5	1346,1	562000,51	430594,32	K
T05rorf	14,871	9	10	282	2010	64	22,30617	17	42,94249	1412,9	0,0	-67,5	1345,4	562000,51	430594,32	K
T06nm	16,267	4	5	124	2010	64	24,27303	17	36,59166	1530,3	0,0	-67,6	1462,7	567029,25	434355,96	K
T06nm	13,159	9	10	282	2010	64	24,26872	17	36,60378	1521,9	0,0	-67,6	1454,3	567019,68	434347,73	K
T07nk	12,650	14	3	73	2010	64	25,30623	17	31,16531	1635,6	0,5	-67,7	1565,4	571344,28	436374,12	FS
T07nk	17,050	4	5	124	2010	64	25,30550	17	31,16758	1636,0	-2,1	-67,7	1566,2	571342,49	436372,73	K
T07nk	12,071	9	10	282	2010	64	25,30429	17	31,17761	1629,5	-4,7	-67,7	1557,1	571334,49	436370,28	K
T07rore	12,650	14	3	73	2010	64	25,30623	17	31,16531	1635,6	-3,0	-67,7	1564,9	571344,28	436374,12	FS
T07rorf	12,650	14	3	73	2010	64	25,30623	17	31,16531	1635,6	0,0	-67,7	1567,9	571344,28	436374,12	FS
T07rorf	17,050	4	5	124	2010	64	25,30550	17	31,16758	1636,0	0,0	-67,7	1568,3	571342,49	436372,73	K
T07rorf	10,963	11	6	162	2010	64	25,30514	17	31,16994	1635,9	0,0	-67,7	1568,2	571340,61	436372,00	K
T07rorg	10,963	11	6	162	2010	64	25,30514	17	31,16994	1635,9	-2,8	-67,7	1565,4	571340,61	436372,00	K
T07rorg	12,071	9	10	282	2010	64	25,30429	17	31,17761	1629,5	2,0	-67,7	1563,8	571334,49	436370,28	K
T07rorh	12,071	9	10	282	2010	64	25,30429	17	31,17761	1629,5	0,0	-67,7	1561,8	571334,49	436370,28	K
T08nm	18,042	4	5	124	2010	64	26,30260	17	27,79821	1707,0	0,0	-67,8	1639,2	574002,93	438289,36	K
T08nm	11,017	9	10	282	2010	64	26,30196	17	27,79944	1701,7	0,0	-67,8	1634,0	574001,97	438288,16	K

Appendix D: Measured surface velocity on Vatnajökull in 2010.

Site	date	Calendar day #	date	Calendar day #	# of days	translation (m)	(°)	velocity (cm/day)	(m/annum)
BORad	20090604	155	20091016	289	134	6,11	205	4,56	16,66
BORTHNb	20080928	272	20090209	40	133	2,28	218	1,71	6,26
BORTHNb	20090209	40	20090517	137	97	0,82	186	0,84	3,08
B07p	20100508	128	20101007	280	152	1,24	147	0,81	2,97
B08q	20091014	287	20100506	126	204	1,86	73	0,91	3,32
B08q	20100506	126	20101007	280	154	0,28	23	0,18	0,67
B09q	20091014	287	20100506	126	204	1,49	51	0,73	2,66
B09q	20100506	126	20101007	280	154	0,58	352	0,38	1,37
B10r	20100506	126	20101007	280	154	1,03	346	0,67	2,45
B12p	20100506	126	20101007	280	154	19,69	22	12,79	46,67
B13p	20100505	125	20101007	280	155	23,07	26	14,88	54,33
B14p	20080719	201	20101007	280	809	63,75	38	7,88	28,76
B14r	20100505	125	20101008	281	156	17,96	33	11,51	42,02
B15e	20100505	125	20101007	280	155	13,41	48	8,65	31,59
B16r	20100505	125	20101008	281	156	4,82	215	3,09	11,27
B17p	20100506	126	20101007	280	154	14,16	15	9,20	33,57
B18m	20091013	286	20101006	279	358	27,49	345	7,68	28,03
B19n	20100507	127	20101006	279	152	1,44	131	0,95	3,46
BB0o	20100508	128	20101006	279	151	0,55	242	0,37	1,34
BORTHNb	20091016	289	20100314	73	149	12,50	183	8,39	30,63
BORTHNb	20100314	73	20100510	130	57	3,88	184	6,81	24,84
BORTHNb	20100510	130	20100606	157	27	2,54	140	9,40	34,30
BORTHNb	20100606	157	20101010	283	126	16,06	185	12,75	46,52
BORTHNb	20101010	283	20110111	11	93	3,24	189	3,48	12,72
Br1d	20090829	241	20100130	30	154	3,54	180	2,30	8,38
Br1e	20100130	30	20100823	235	205	4,50	178	2,20	8,02
Br1e	20100823	235	20101013	286	51	0,73	170	1,44	5,24
Br2f	20090829	241	20100130	30	154	10,68	167	6,94	25,32
Br2g	20100130	30	20101013	286	256	9,26	180	3,62	13,20
Br3l	20090829	241	20100130	30	154	16,10	154	10,45	38,16
Br3m	20100130	30	20101013	286	256	26,00	160	10,16	37,07
Br7n	20100508	128	20101012	285	157	42,08	175	26,80	97,82
Bruo	20100506	126	20101006	279	153	1,67	345	1,09	3,97
Budo	20100506	126	20101006	279	153	21,77	3	14,23	51,94
D05m	20100508	128	20101011	284	156	12,64	37	8,10	29,57
D07h	20060926	269	20101011	284	1475	179,11	21	12,14	44,32
D07k	20080930	274	20101011	284	740	93,49	22	12,63	46,11
D07m	20100509	129	20101011	284	155	25,04	23	16,16	58,97
D09l	20091016	289	20101011	284	360	15,99	350	4,44	16,21
D09m	20100509	129	20101011	284	155	7,51	351	4,85	17,69
D12n	20100508	128	20101008	281	153	0,71	352	0,46	1,70
E01o	20100507	127	20101007	280	153	0,34	15	0,23	0,82
E02o	20100507	127	20101007	280	153	18,32	11	11,97	43,70
E03o	20090515	135	20101007	280	510	27,13	346	5,32	19,42
E03STIKp	20100507	127	20101007	280	153	9,83	342	6,43	23,46
E03VIRp	20100507	127	20101007	280	153	8,85	350	5,79	21,12
E04o	20100507	127	20101007	280	153	1,16	28	0,76	2,76

Fl01a	20100507	127	20101006	279	152	19,26	135	12,67	46,26
G02g	20100608	159	20101010	283	124	6,12	200	4,93	18,01
G03h	20100608	159	20101010	283	124	19,03	189	15,34	56,00
G04o	20100608	159	20101010	283	124	14,49	183	11,68	42,64
gb2rora	20091013	286	20100506	126	205	11,91	354	5,81	21,21
gb2c	20091013	286	20100506	126	205	11,91	354	5,81	21,21
gb2c	20100506	126	20101006	279	153	14,34	354	9,37	34,21
Go1m	20090718	199	20101010	283	449	4,81	155	1,07	3,91
Go1n	20100509	129	20101010	283	154	4,11	181	2,67	9,75
HAABj	20100609	160	20101010	283	123	0,59	341	0,48	1,75
Hof01h	20100507	127	20101007	280	153	14,19	173	9,28	33,86
Hosp1f	20100129	29	20100824	236	207	15,16	163	7,33	26,74
K01q	20100509	129	20101011	284	155	2,26	304	1,46	5,32
K02r	20100509	129	20101011	284	155	10,06	300	6,49	23,70
K04r	20100509	129	20101011	284	155	21,79	289	14,06	51,31
K05q	20091016	289	20101010	283	359	31,92	245	8,89	32,46
K05r	20100509	129	20101010	283	154	14,84	245	9,64	35,18
K06q	20100608	159	20101010	283	124	3,73	194	3,01	10,97
K07m	20100509	129	20101011	284	155	6,44	265	4,15	15,16
S02i	20100511	131	20110111	11	245	22,11	193	9,03	32,94
S04j	20100510	130	20101010	283	153	22,89	204	14,96	54,61
Skf01a	20100508	128	20101006	279	151	13,43	111	8,90	32,47
T01nm	20100504	124	20110111	11	252	0,55	190	0,22	0,79
T02nm	20100504	124	20110111	11	252	8,52	272	3,38	12,33
T03nm	20100504	124	20101009	282	158	11,96	249	7,57	27,64
T04nm	20100504	124	20100605	156	32	2,75	243	8,60	31,39
T04nm	20100605	156	20101009	282	126	10,41	238	8,27	30,17
T05nl	20091016	289	20100313	72	148	7,49	236	5,06	18,48
T05nl	20100313	72	20100504	124	52	1,88	229	3,61	13,17
T05nl	20100504	124	20101009	282	158	10,42	227	6,60	24,07
T05nl	20101009	282	20110111	11	94	4,48	235	4,77	17,40
T05rord	20091016	289	20100313	72	148	7,49	236	5,06	18,48
T05rord	20100313	72	20100504	124	52	1,88	229	3,61	13,17
T05rord	20100504	124	20100605	156	32	2,07	247	6,46	23,56
T05rord	20100605	156	20100611	162	6	2,58	155	43,01	156,99
T05rore	20100611	162	20101009	282	120	7,89	240	6,58	24,00
T05rorf	20101009	282	20110111	11	94	4,48	235	4,77	17,40
T06nm	20100504	124	20101009	282	158	12,59	231	7,97	29,09
T07nk	20091016	289	20100314	73	149	7,59	235	5,10	18,60
T07nk	20100314	73	20100504	124	51	2,27	233	4,45	16,24
T07nk	20100504	124	20101009	282	158	8,36	254	5,29	19,31
T07nk	20101009	282	20110111	11	94	4,30	235	4,58	16,71
T07rore	20091016	289	20100314	73	149	7,59	235	5,10	18,60
T07rorf	20100314	73	20100504	124	51	2,27	233	4,45	16,24
T07rorf	20100504	124	20100611	162	38	2,01	251	5,29	19,29
T07rorg	20100611	162	20101009	282	120	6,36	256	5,30	19,33
T07rorh	20101009	282	20110111	11	94	4,30	235	4,58	16,71
T08nm	20100504	124	20101009	282	158	1,54	220	0,98	3,56

Appendix E: Melt water runoff to selected rivers in summer 2010, derived from summer balance.

ΔS: area in a given elevation range where summer balance is negative, **$\sum\Delta S$**: cumulative area above a given elevation, **ΔQ_s**: melt water runoff from a given elevation range, **$\sum\Delta Q_s$** : cumulative melt water runoff from an area above given elevation.

Tungnaá water drainage basin

Elevation (m a. s. l.)		ΔS km^2	$\sum\Delta S$ km^2	ΔQ_s $(10^6 m^3)$	$\sum\Delta Q_s$ $(10^6 m^3)$
1350	1400	0,6	0,6	2,1	2,1
1300	1350	6,2	6,8	23,2	25,3
1250	1300	10,7	17,5	41,2	66,5
1200	1250	11,4	28,9	46,3	112,9
1150	1200	10,8	39,7	46,7	159,6
1100	1150	12,8	52,5	59,5	219,1
1050	1100	11,9	64,4	60,0	279,1
1000	1050	9,7	74,1	51,3	330,4
950	1000	10,8	84,9	60,1	390,4
900	950	9,0	93,9	52,9	443,3
850	900	8,3	102,2	51,2	494,6
800	850	8,6	110,8	54,9	549,5
750	800	6,3	117,1	42,0	591,5
700	750	4,2	121,3	29,1	620,6
650	700	0,5	121,8	4,0	624,5

Sylgja water drainage basin

Elevation (m a. s. l.)		ΔS km^2	$\sum\Delta S$ km^2	ΔQ_s $(10^6 m^3)$	$\sum\Delta Q_s$ $(10^6 m^3)$
1300	1350	1,3	1,3	5,0	5,0
1250	1300	3,6	4,9	14,2	19,2
1200	1250	6,4	11,3	26,1	45,3
1150	1200	8,3	19,6	35,3	80,6
1100	1150	6,6	26,2	29,6	110,2
1050	1100	7,6	33,8	37,3	147,4
1000	1050	3,8	37,6	20,7	168,1
950	1000	1,5	39,1	8,3	176,4
900	950	0,6	39,7	3,4	179,7
850	900	0,0	39,7	0,1	179,9

Western Skaftá cauldron water drainage basin

Elevation (m a. s. l.)		ΔS km^2	$\sum\Delta S$ km^2	ΔQ_s $(10^6 m^3)$	$\sum\Delta Q_s$ $(10^6 m^3)$
1700	1750	3,2	3,2	10,7	10,7
1650	1700	7,0	10,2	24,4	35,1
1600	1650	8,4	18,6	29,8	64,9
1550	1600	5,0	23,6	17,7	82,6
1500	1550	1,5	25,1	5,1	87,7

Eastern Skaftár cauldoron water drainage basin

Elevation (m a. s. l.)		ΔS km^2	$\sum\Delta S$ km^2	ΔQ_s $(10^6 m^3)$	$\sum\Delta Q_s$ $(10^6 m^3)$
1750	1800	2,5	2,5	6,6	6,6
1700	1750	10,6	13,1	31,0	37,6
1650	1700	14,8	27,9	46,1	83,7
1600	1650	9,3	37,2	31,7	115,3
1550	1600	2,2	39,4	7,6	123,0

Grímsvötn water drainage basin

Elevation (m a. s. l.)		ΔS km^2	$\sum\Delta S$ km^2	ΔQ_s $(10^6 m^3)$	$\sum\Delta Q_s$ $(10^6 m^3)$
1900	1950	0,6	0,6	1,1	1,1
1850	1900	1,3	1,9	2,4	3,5
1800	1850	1,6	3,5	3,5	7,0
1750	1800	3,9	7,4	9,5	16,5
1700	1750	15,9	23,3	36,6	53,1
1650	1700	56,4	79,7	116,6	169,7
1600	1650	30,9	110,6	81,0	250,7
1550	1600	18,7	129,3	50,4	301,1
1500	1550	16,7	146,0	49,3	350,3
1450	1500	11,6	157,6	38,4	388,7
1400	1450	15,1	172,7	52,7	441,4
1350	1400	0,6	173,3	2,2	443,7

Kaldakvísl water drainage basin

Elevation (m a. s. l.)		ΔS km^2	$\sum\Delta S$ km^2	ΔQ_s $(10^6 m^3)$	$\sum\Delta Q_s$ $(10^6 m^3)$
1950	2000	4,8	4,8	7,2	7,2
1900	1950	12,9	17,7	22,1	29,3
1850	1900	6,4	24,1	14,4	43,8
1800	1850	6,4	30,5	16,6	60,3
1750	1800	11,7	42,2	32,9	93,2
1700	1750	21,1	63,3	69,6	162,8
1650	1700	16,7	80,0	59,9	222,6
1600	1650	14,2	94,2	51,9	274,5
1550	1600	19,4	113,6	71,6	346,1
1500	1550	27,2	140,8	96,6	442,7
1450	1500	28,5	169,3	105,2	547,8
1400	1450	23,1	192,4	88,9	636,7
1350	1400	21,6	214,0	86,6	723,3
1300	1350	21,3	235,3	89,7	813,0
1250	1300	22,6	257,9	99,1	912,1
1200	1250	22,6	280,5	105,6	1017,7
1150	1200	20,2	300,7	100,3	1118,0
1100	1150	18,3	319,0	96,7	1214,7
1050	1100	17,2	336,2	96,0	1310,7
1000	1050	14,9	351,1	88,5	1399,1
950	1000	10,7	361,8	67,8	1466,9
900	950	5,6	367,4	36,9	1503,8
850	900	0,5	367,9	3,6	1507,4

Jökulsá á Fjöllum water drainage basin

Elevation (m a. s. l.)		ΔS km^2	$\sum\Delta S$ km^2	ΔQ_s $(10^6 m^3)$	$\sum\Delta Q_s$ $(10^6 m^3)$
2000	2050	0,0	0,0	0,0	0,0
1950	2000	8,2	8,2	10,3	10,3
1900	1950	25,6	33,8	31,7	42,0
1850	1900	18,4	52,2	24,9	66,9
1800	1850	14,6	66,8	18,7	85,6
1750	1800	22,3	89,1	34,1	119,7
1700	1750	34,2	123,3	53,3	173,0
1650	1700	79,5	202,8	123,1	296,1
1600	1650	116,5	319,3	206,5	502,6
1550	1600	100,9	420,2	209,9	712,5
1500	1550	97,7	517,9	215,3	927,8
1450	1500	85,7	603,6	195,8	1123,7
1400	1450	74,3	677,9	175,8	1299,5
1350	1400	60,2	738,1	150,1	1449,5
1300	1350	49,1	787,2	132,1	1581,6
1250	1300	52,5	839,7	159,0	1740,6
1200	1250	57,4	897,1	202,8	1943,4
1150	1200	54,5	951,6	222,9	2166,3
1100	1150	45,9	997,5	204,9	2371,3
1050	1100	34,1	1031,6	162,6	2533,9
1000	1050	36,4	1068,0	186,2	2720,1
950	1000	31,5	1099,5	173,1	2893,2
900	950	26,2	1125,7	152,7	3045,9
850	900	25,4	1151,1	154,9	3200,9
800	850	20,2	1171,3	128,9	3329,8
750	800	15,2	1186,5	103,1	3432,9
700	750	1,7	1188,2	12,2	3445,1

Kreppa and Kverká water drainage basin

Elevation (m a. s. l.)		ΔS km²	ΣΔS km²	ΔQ_s ($10^6 m^3$)	$\Sigma\Delta Q_s$ ($10^6 m^3$)
1850	1900	1,0	1,0	1,0	1,0
1800	1850	4,2	5,2	3,7	4,7
1750	1800	2,8	8,0	2,8	7,5
1700	1750	3,6	11,6	4,7	12,2
1650	1700	5,0	16,6	7,1	19,2
1600	1650	37,9	54,5	63,5	82,8
1550	1600	22,6	77,1	39,9	122,7
1500	1550	14,2	91,3	27,2	149,9
1450	1500	15,4	106,7	31,2	181,1
1400	1450	19,3	126,0	40,9	222,1
1350	1400	25,2	151,2	54,9	277,0
1300	1350	20,5	171,7	47,0	324,0
1250	1300	16,4	188,1	40,6	364,6
1200	1250	18,1	206,2	50,6	415,3
1150	1200	18,2	224,4	56,8	472,0
1100	1150	17,5	241,9	59,1	531,1
1050	1100	11,6	253,5	42,1	573,2
1000	1050	14,1	267,6	56,8	630,0
950	1000	16,1	283,7	72,3	702,2
900	950	14,4	298,1	69,7	772,0
850	900	14,5	312,6	74,6	846,6
800	850	11,5	324,1	61,6	908,2
750	800	9,3	333,4	52,7	960,9
700	750	4,2	337,6	24,9	985,7
650	700	0,4	338,0	2,7	988,4

Jökulsá á Brú water drainage basin

Elevation (m a. s. l.)		ΔS km²	ΣΔS km²	ΔQ_s ($10^6 m^3$)	$\Sigma\Delta Q_s$ ($10^6 m^3$)
1600	1650	8,3	8,3	14,0	14,0
1550	1600	30,4	38,7	52,1	66,1
1500	1550	60,6	99,3	110,2	176,4
1450	1500	63,6	162,9	128,7	305,1
1400	1450	95,6	258,5	184,3	489,4
1350	1400	124,5	383,0	236,7	726,1
1300	1350	133,2	516,2	269,6	995,8
1250	1300	128,3	644,5	292,2	1287,9
1200	1250	102,8	747,3	263,3	1551,3
1150	1200	87,3	834,6	247,2	1798,5
1100	1150	69,3	903,9	218,8	2017,2
1050	1100	61,8	965,7	221,2	2238,4
1000	1050	51,8	1017,5	207,5	2445,9
950	1000	43,4	1060,9	191,6	2637,6
900	950	34,6	1095,5	165,8	2803,4
850	900	30,4	1125,9	155,4	2958,8
800	850	29,9	1155,8	163,1	3121,9
750	800	26,8	1182,6	154,8	3276,7
700	750	19,6	1202,2	117,4	3394,1
650	700	12,3	1214,5	75,4	3469,5
600	650	0,3	1214,8	2,0	3471,5

Jökulsá á Fljótsdal water drainage basin

Elevation (m a. s. l.)		ΔS km^2	ΣΔS km^2	ΔQ_s $(10^6 m^3)$	$\Sigma\Delta Q_s$ $(10^6 m^3)$
1500	1550	0,0	0,0	0,1	0,1
1450	1500	0,9	0,9	1,3	1,4
1400	1450	1,9	2,8	2,8	4,2
1350	1400	2,8	5,6	4,7	8,9
1300	1350	5,2	10,8	9,6	18,5
1250	1300	15,8	26,6	33,8	52,3
1200	1250	15,9	42,5	39,0	91,4
1150	1200	17,6	60,1	49,2	140,5
1100	1150	15,1	75,2	47,9	188,4
1050	1100	12,7	87,9	45,4	233,8
1000	1050	11,9	99,8	48,1	281,9
950	1000	9,0	108,8	40,0	322,0
900	950	5,8	114,6	27,4	349,4
850	900	4,3	118,9	21,5	370,9
800	850	3,3	122,2	17,3	388,2
750	800	3,4	125,6	18,6	406,8
700	750	3,3	128,9	19,2	426,0
650	700	1,7	130,6	10,4	436,4

Hornafjarðarfljót water drainage basin

Elevation (m a. s. l.)		ΔS km^2	∑ΔS km^2	ΔQ_s $(10^6 m^3)$	$\sum \Delta Q_s$ $(10^6 m^3)$
1450	1500	1,0	1,0	1,3	1,3
1400	1450	7,4	8,4	11,4	12,7
1350	1400	12,2	20,6	21,2	33,9
1300	1350	18,3	38,9	35,6	69,5
1250	1300	36,6	75,5	79,7	149,2
1200	1250	30,2	105,7	70,6	219,8
1150	1200	20,8	126,5	54,7	274,4
1100	1150	19,8	146,3	58,1	332,6
1050	1100	15,3	161,6	49,2	381,8
1000	1050	11,7	173,3	40,0	421,8
950	1000	11,1	184,4	41,0	462,9
900	950	8,2	192,6	33,5	496,4
850	900	5,5	198,1	24,4	520,8
800	850	4,4	202,5	20,4	541,2
750	800	4,1	206,6	20,2	561,4
700	750	4,0	210,6	20,5	581,9
650	700	3,5	214,1	18,3	600,3
600	650	2,6	216,7	13,9	614,1
550	600	2,0	218,7	11,0	625,1
500	550	1,8	220,5	10,2	635,3
450	500	1,4	221,9	8,0	643,3
400	450	1,3	223,2	7,6	651,0
350	400	0,8	224,0	5,0	656,0
300	350	1,1	225,1	7,4	663,3
250	300	2,3	227,4	16,3	679,6
200	250	3,5	230,9	26,5	706,1
150	200	2,7	233,6	22,0	728,2
100	150	2,1	235,7	18,8	746,9
50	100	2,8	238,5	26,4	773,3
0	50	0,6	239,1	5,3	778,6

Jökulsá á Breiðamerkursandi water drainage basin

Elevation (m a. s. l.)		ΔS km^2	∑ΔS km^2	ΔQ_s ($10^6 m^3$)	$\sum\Delta Q_s$ ($10^6 m^3$)
1700	1750	0,8	0,8	0,7	0,7
1650	1700	4,0	4,8	3,9	4,5
1600	1650	12,9	17,7	14,8	19,4
1550	1600	19,1	36,8	25,8	45,1
1500	1550	23,0	59,8	38,5	83,6
1450	1500	35,2	95,0	63,7	147,3
1400	1450	49,6	144,6	97,0	244,3
1350	1400	83,3	227,9	177,8	422,1
1300	1350	85,4	313,3	207,3	629,4
1250	1300	53,1	366,4	148,2	777,6
1200	1250	35,1	401,5	106,6	884,2
1150	1200	28,9	430,4	93,0	977,2
1100	1150	24,6	455,0	83,9	1061,2
1050	1100	20,7	475,7	73,8	1135,0
1000	1050	17,8	493,5	66,5	1201,5
950	1000	19,0	512,5	73,8	1275,3
900	950	20,2	532,7	81,3	1356,6
850	900	20,5	553,2	85,8	1442,5
800	850	20,2	573,4	87,7	1530,2
750	800	19,5	592,9	89,3	1619,4
700	750	21,1	614,0	100,0	1719,5
650	700	26,7	640,7	129,4	1848,8
600	650	18,5	659,2	94,7	1943,5
550	600	18,5	677,7	99,1	2042,6
500	550	7,0	684,7	38,2	2080,7
450	500	7,7	692,4	43,5	2124,3
400	450	5,8	698,2	34,0	2158,3
350	400	5,5	703,7	33,3	2191,6
300	350	6,5	710,2	42,3	2233,9
250	300	6,0	716,2	43,3	2277,2
200	250	6,3	722,5	52,4	2329,6
150	200	5,1	727,6	46,5	2376,1
100	150	5,1	732,7	48,8	2424,8
50	100	4,1	736,8	40,6	2465,4
0	50	2,7	739,5	26,9	2492,3

Breiðárlón/Fjallsárlón water drainage basin

Elevation (m a. s. l.)		ΔS km^2	∑ΔS km^2	ΔQ_s $(10^6 m^3)$	$\sum \Delta Q_s$ $(10^6 m^3)$
1900	1950	0,1	0,1	0,0	0,0
1850	1900	1,4	1,5	0,0	0,1
1800	1850	2,1	3,6	0,4	0,5
1750	1800	2,5	6,1	0,9	1,4
1700	1750	2,9	9,0	1,6	3,0
1650	1700	2,9	11,9	2,2	5,2
1600	1650	4,0	15,9	3,8	9,0
1550	1600	4,2	20,1	4,9	13,9
1500	1550	6,0	26,1	7,9	21,8
1450	1500	5,0	31,1	7,3	29,0
1400	1450	5,3	36,4	8,9	37,9
1350	1400	6,4	42,8	13,0	50,9
1300	1350	12,6	55,4	30,3	81,2
1250	1300	6,7	62,1	17,8	98,9
1200	1250	5,6	67,7	16,2	115,1
1150	1200	5,1	72,8	16,1	131,2
1100	1150	4,5	77,3	15,4	146,5
1050	1100	5,0	82,3	17,6	164,1
1000	1050	6,0	88,3	21,6	185,8
950	1000	7,0	95,3	26,8	212,6
900	950	8,4	103,7	33,9	246,5
850	900	6,7	110,4	28,6	275,1
800	850	8,4	118,8	37,2	312,3
750	800	8,8	127,6	40,9	353,2
700	750	6,1	133,7	29,3	382,5
650	700	7,4	141,1	36,6	419,2
600	650	8,3	149,4	42,7	461,8
550	600	8,8	158,2	47,1	508,9
500	550	9,5	167,7	51,6	560,5
450	500	9,6	177,3	53,8	614,3
400	450	11,1	188,4	64,5	678,8
350	400	8,5	196,9	51,9	730,7
300	350	7,7	204,6	49,8	780,5
250	300	7,4	212,0	53,1	833,6
200	250	6,8	218,8	54,5	888,1
150	200	4,6	223,4	41,1	929,2
100	150	4,3	227,7	41,2	970,4
50	100	3,7	231,4	36,4	1006,8
0	50	1,8	233,2	18,2	1025,0

Skeiðarársandur water drainage basin

Elevation (m a. s. l.)		ΔS km^2	$\sum \Delta S$ km^2	ΔQ_s ($10^6 m^3$)	$\sum \Delta Q_s$ ($10^6 m^3$)
1700	1750	1,2	1,2	1,5	1,5
1650	1700	20,5	21,7	34,9	36,5
1600	1650	76,2	97,9	124,5	161,0
1550	1600	84,6	182,5	139,7	300,6
1500	1550	104,1	286,6	179,3	479,9
1450	1500	97,6	384,2	176,7	656,6
1400	1450	95,1	479,3	181,9	838,5
1350	1400	83,3	562,6	174,5	1013,0
1300	1350	71,9	634,5	169,2	1182,2
1250	1300	62,8	697,3	165,6	1347,8
1200	1250	52,9	750,2	154,7	1502,5
1150	1200	44,9	795,1	143,1	1645,6
1100	1150	36,1	831,2	122,1	1767,6
1050	1100	29,5	860,7	105,0	1872,7
1000	1050	25,0	885,7	92,1	1964,8
950	1000	25,0	910,7	96,4	2061,2
900	950	24,8	935,5	100,3	2161,5
850	900	27,8	963,3	116,7	2278,2
800	850	22,5	985,8	98,7	2376,9
750	800	19,6	1005,4	89,9	2466,8
700	750	19,1	1024,5	90,8	2557,6
650	700	11,9	1036,4	57,9	2615,5
600	650	13,1	1049,5	65,5	2681,0
550	600	12,4	1061,9	63,2	2744,2
500	550	8,3	1070,2	43,7	2788,0
450	500	5,5	1075,7	30,2	2818,1
400	450	6,7	1082,4	37,6	2855,7
350	400	11,1	1093,5	63,5	2919,2
300	350	14,2	1107,7	86,7	3005,9
250	300	15,3	1123,0	100,6	3106,5
200	250	12,4	1135,4	88,7	3195,3
150	200	11,3	1146,7	86,1	3281,4
100	150	13,5	1160,2	110,0	3391,4
50	100	5,0	1165,2	42,6	3434,0

Súla water drainage basin

Elevation (m a. s. l.)		ΔS km^2	∑ΔS km^2	ΔQ_s $(10^6 m^3)$	$\sum\Delta Q_s$ $(10^6 m^3)$
1700	1750	0,5	0,5	1,1	1,1
1650	1700	1,4	1,9	2,8	3,9
1600	1650	2,6	4,5	5,2	9,1
1550	1600	4,1	8,6	8,6	17,8
1500	1550	5,9	14,5	13,3	31,0
1450	1500	11,4	25,9	27,7	58,8
1400	1450	11,1	37,0	26,5	85,2
1350	1400	9,3	46,3	22,2	107,5
1300	1350	8,2	54,5	20,4	127,9
1250	1300	6,7	61,2	17,6	145,5
1200	1250	8,1	69,3	22,9	168,4
1150	1200	9,2	78,5	28,4	196,8
1100	1150	15,6	94,1	52,1	249,0
1050	1100	15,9	110,0	56,7	305,7
1000	1050	16,5	126,5	62,1	367,7
950	1000	18,7	145,2	73,8	441,5
900	950	15,3	160,5	62,7	504,2
850	900	12,1	172,6	51,7	555,9
800	850	11,7	184,3	51,6	607,6
750	800	7,0	191,3	32,2	639,8
700	750	6,0	197,3	28,8	668,5
650	700	4,9	202,2	24,1	692,6
600	650	9,0	211,2	45,5	738,1
550	600	11,7	222,9	60,8	798,9
500	550	8,9	231,8	47,7	846,5
450	500	7,2	239,0	39,3	885,9
400	450	6,3	245,3	35,0	920,9
350	400	4,8	250,1	27,2	948,1
300	350	1,8	251,9	11,0	959,0
250	300	0,9	252,8	6,2	965,3
200	250	0,8	253,6	5,6	970,9
150	200	0,8	254,4	6,2	977,1
100	150	0,8	255,2	7,0	984,0
50	100	0,6	255,8	5,8	989,8

Djúpá water drainage basin

Elevation (m a. s. l.)		ΔS km^2	∑ΔS km^2	$ΔQ_s$ $(10^6 m^3)$	$∑ΔQ_s$ $(10^6 m^3)$
1450	1500	0,1	0,1	0,3	0,3
1400	1450	0,3	0,3	0,9	1,2
1350	1400	0,9	0,9	2,5	3,7
1300	1350	3,8	3,8	11,6	15,2
1250	1300	3,3	3,3	9,9	25,2
1200	1250	2,9	2,9	9,6	34,7
1150	1200	3,5	3,5	12,6	47,3
1100	1150	5,3	5,3	20,5	67,8
1050	1100	7,0	7,0	31,3	99,1
1000	1050	9,8	9,8	49,3	148,5
950	1000	8,0	8,0	42,4	190,8
900	950	8,1	8,1	42,6	233,4
850	900	7,5	7,5	39,8	273,2
800	850	9,1	9,1	49,2	322,4
750	800	6,7	6,7	37,7	360,1
700	750	4,0	4,0	24,0	384,1
650	700	3,0	3,0	18,6	402,7
600	650	0,4	0,4	2,7	405,4

Brunná water drainage basin

Elevation (m a. s. l.)		ΔS km^2	∑ΔS km^2	$ΔQ_s$ $(10^6 m^3)$	$∑ΔQ_s$ $(10^6 m^3)$
1050	1100	0,0	0,0	0,4	0,4
1000	1050	1,1	1,1	6,4	6,8
950	1000	3,3	4,4	18,4	25,2
900	950	4,2	8,6	22,5	47,7
850	900	4,3	12,9	23,3	71,0
800	850	4,9	17,8	26,0	97,0
750	800	5,4	23,2	30,6	127,6
700	750	6,4	29,6	38,2	165,8
650	700	3,9	33,5	24,6	190,4
600	650	2,3	35,8	15,3	205,7
550	600	0,0	35,8	0,2	205,9

Hverfisfljót water drainage basin

Elevation (m a. s. l.)		ΔS km^2	∑ΔS km^2	ΔQ_s ($10^6 m^3$)	$\sum\Delta Q_s$ ($10^6 m^3$)
1700	1750	0,8	0,8	1,7	1,7
1650	1700	5,1	5,9	13,0	14,7
1600	1650	9,1	15,0	26,5	41,1
1550	1600	9,0	24,0	26,7	67,9
1500	1550	19,7	43,7	61,0	128,9
1450	1500	42,0	85,7	136,1	265,0
1400	1450	28,5	114,2	99,5	364,5
1350	1400	24,5	138,7	86,4	451,0
1300	1350	22,9	161,6	82,0	533,0
1250	1300	18,6	180,2	67,8	600,7
1200	1250	20,2	200,4	73,3	674,0
1150	1200	14,1	214,5	52,4	726,4
1100	1150	10,9	225,4	48,1	774,6
1050	1100	10,2	235,6	52,1	826,7
1000	1050	9,3	244,9	52,9	879,6
950	1000	9,4	254,3	52,6	932,2
900	950	8,9	263,2	47,9	980,1
850	900	7,4	270,6	40,3	1020,4
800	850	9,3	279,9	50,6	1071,0
750	800	11,5	291,4	65,2	1136,1
700	750	13,7	305,1	82,1	1218,2
650	700	7,8	312,9	49,3	1267,5
600	650	4,6	317,5	29,7	1297,3
550	600	0,2	317,7	1,2	1298,5

Skaftá water drainage basin

Elevation (m a. s. l.)		ΔS km^2	∑ΔS km^2	ΔQ_s ($10^6 m^3$)	$\sum\Delta Q_s$ ($10^6 m^3$)
1650	1700	2,9	9,5	9,5	3,7
1600	1650	16,1	55,3	64,8	21,6
1550	1600	23,8	82,8	147,6	53,4
1500	1550	29,5	102,9	250,5	93,3
1450	1500	24,1	86,0	336,5	127,3
1400	1450	22,4	81,6	418,1	164,8
1350	1400	20,7	76,1	494,2	207,0
1300	1350	22,9	85,1	579,3	270,9
1250	1300	16,4	62,0	641,3	324,0
1200	1250	21,5	83,6	724,9	408,8
1150	1200	23,9	98,7	823,6	513,0
1100	1150	24,5	111,9	935,5	619,9
1050	1100	26,8	137,2	1072,7	731,6
1000	1050	26,3	142,0	1214,7	844,4
950	1000	20,3	111,0	1325,8	941,1
900	950	15,8	88,6	1414,4	1020,7
850	900	16,2	95,3	1509,6	1105,3
800	850	14,7	91,0	1600,6	1184,7
750	800	11,6	75,4	1676,0	1249,7
700	750	8,5	57,8	1733,8	1299,3
650	700	5,1	35,6	1769,4	1329,6
600	650	0,9	6,4	1775,8	1335,1

Appendix F: MODIS satellite images of Vatnajökull and vicinity 2009-2010.


Left: September 4th 2009; obvious snowfall in the upper regions. Right: September 28th, start of winter.


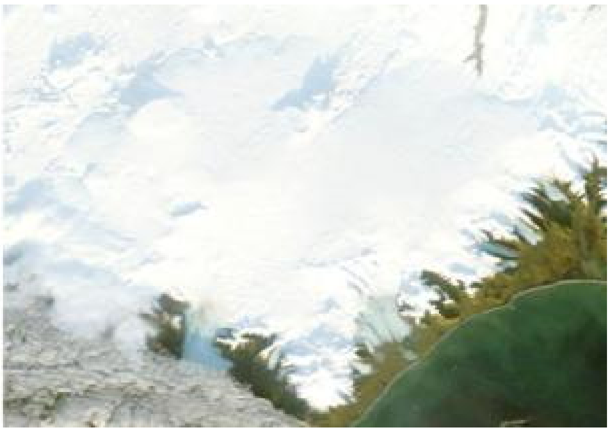

Left: October 27th 2009; still no snow below ~800 m in the south. Right: November 21st, no snow in the lowland below ~600 m, Hálslón is still not frozen over.


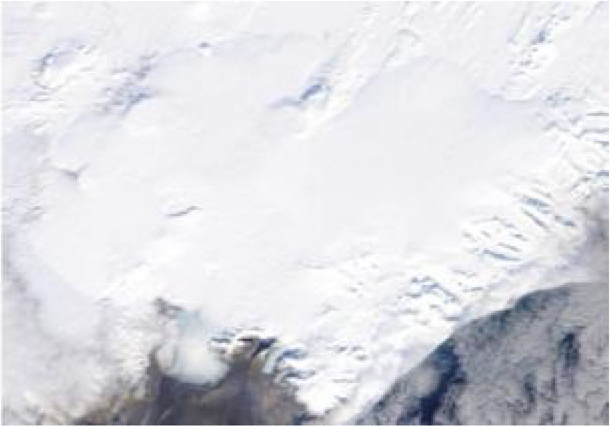

Left: January 29th 2010; still no snow below ~600 m in the south, snow cover north of Dyngjujökull and Kverkfjöll is very thin. Right: March 1st, still almost no snow in the lowland below ~500 m.

Left: April 17th 2010; no snow below ~600 m in the south, the Eyjafjallajökull eruption at full power. In the prevailing northern wind, almost all the tephra in the eruption plume is diverted south over sea.

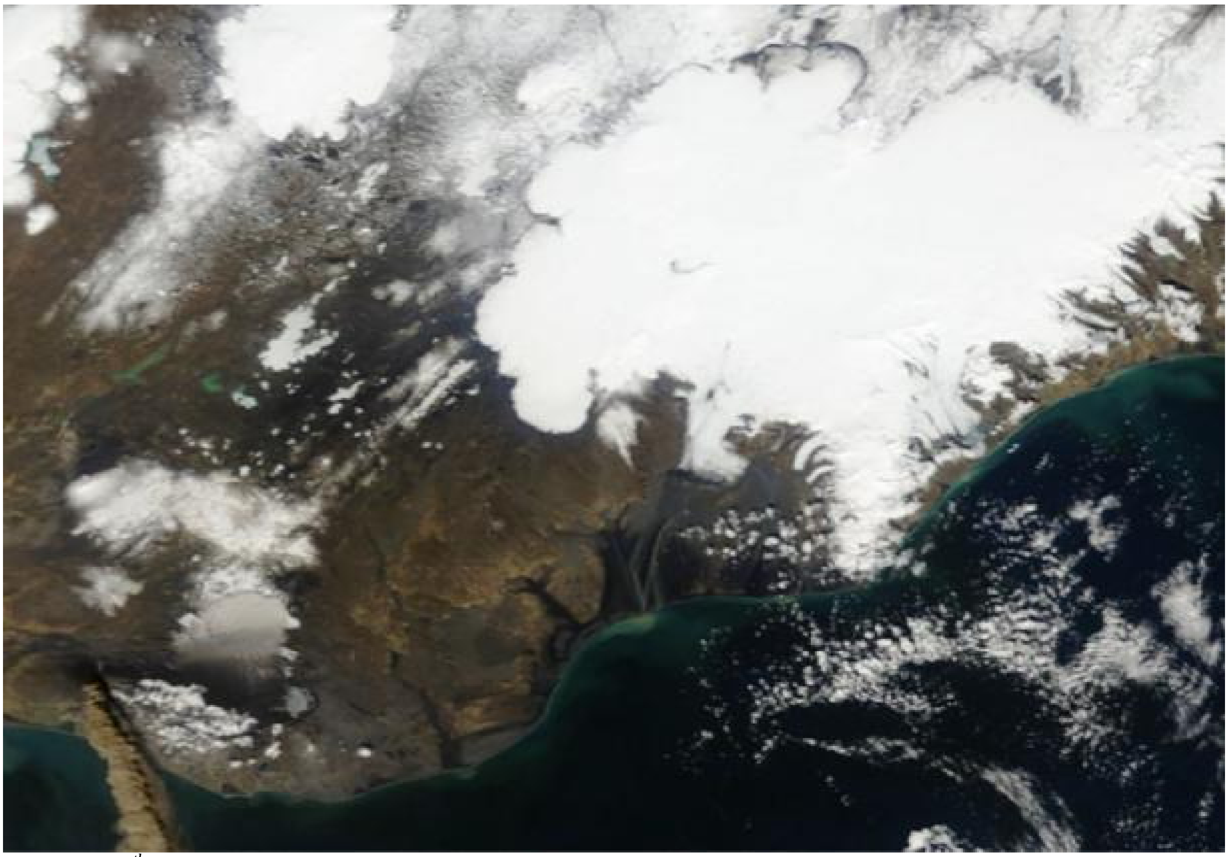

Left: May 11th 2010; after a spell of western wind direction now there is a thick tephra on Mýrdalsjökull, and the brownish surface of Síðujökull indicates slight tephra fallout there. This was also observed on May 10th by the mass balance team working on Siðujökull and Tungnaárjökull .

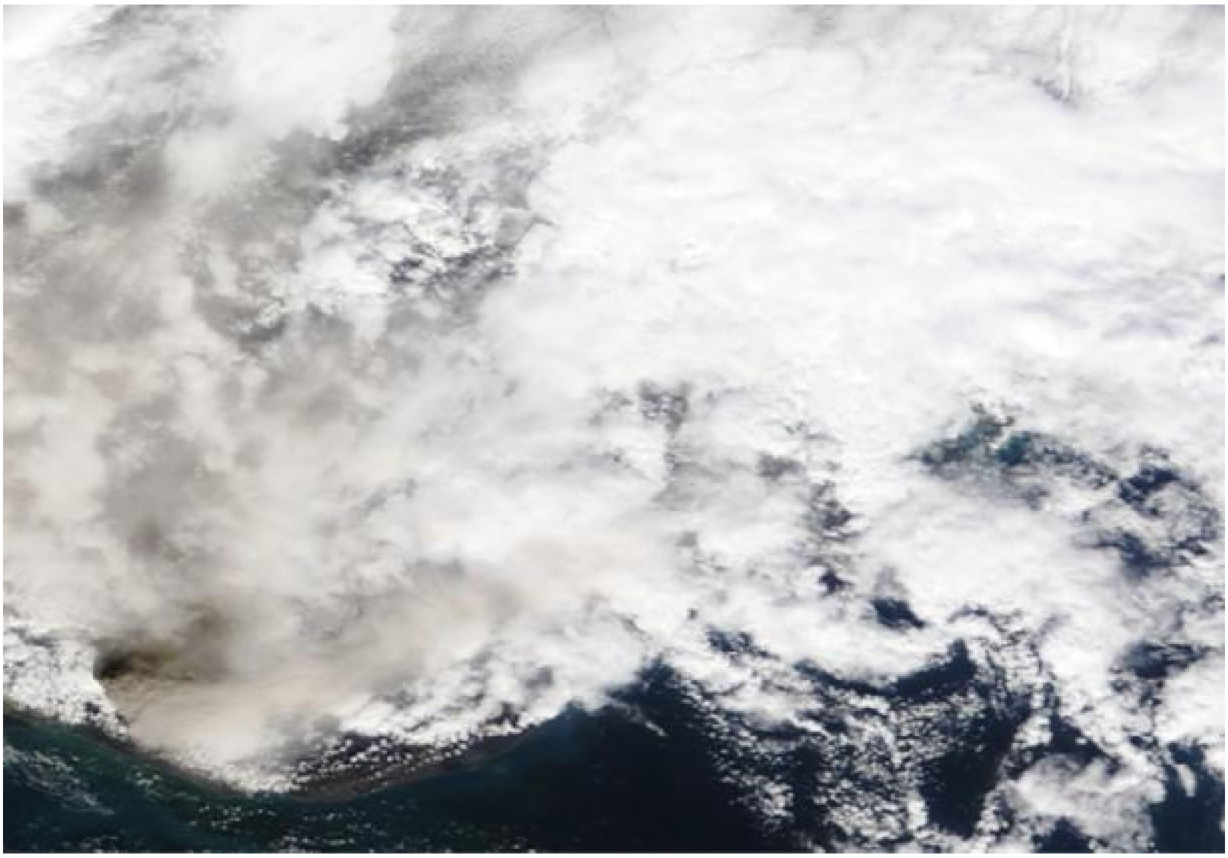

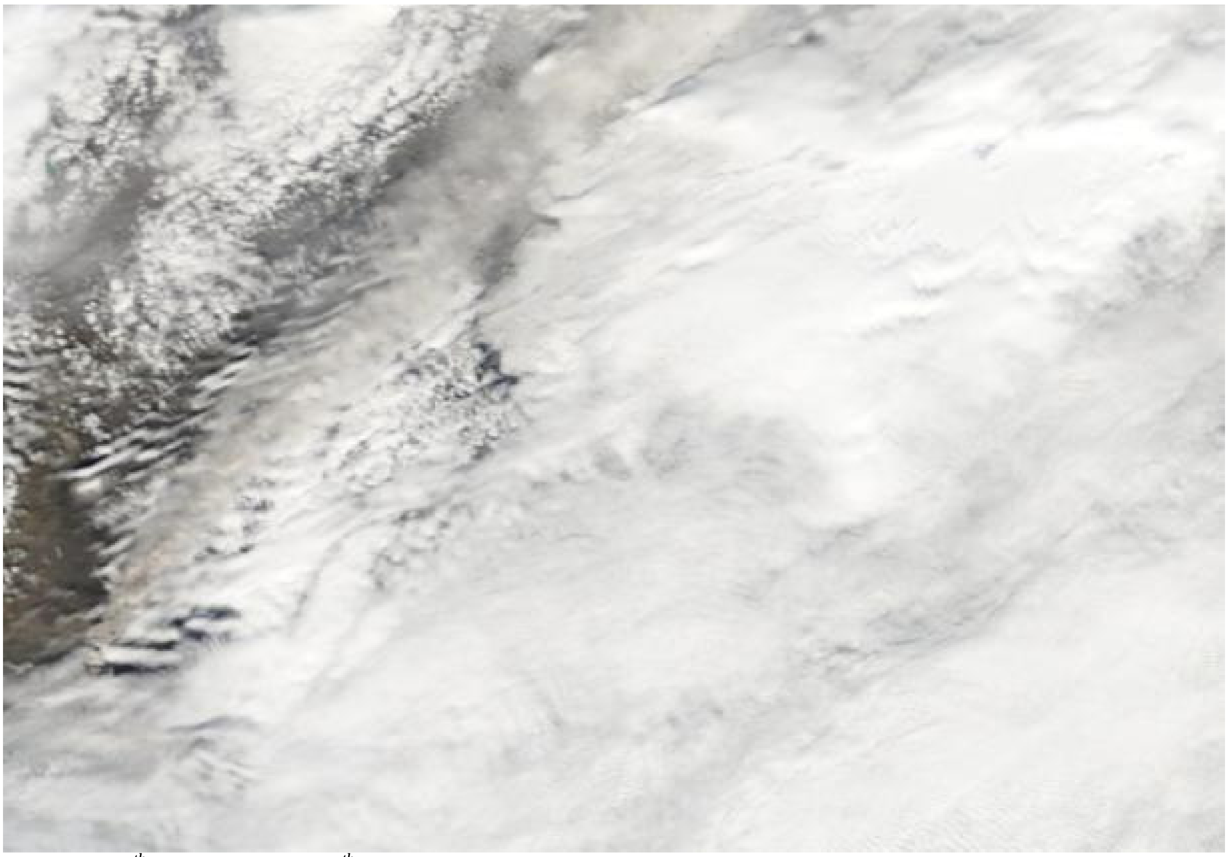

Top: May 17th and bottom May18th. During the last days of the eruption, southern winds were prevailing. This led to thin tephra fallout on Langjökull, Hofsjökull and a large part of Vatnajökull.

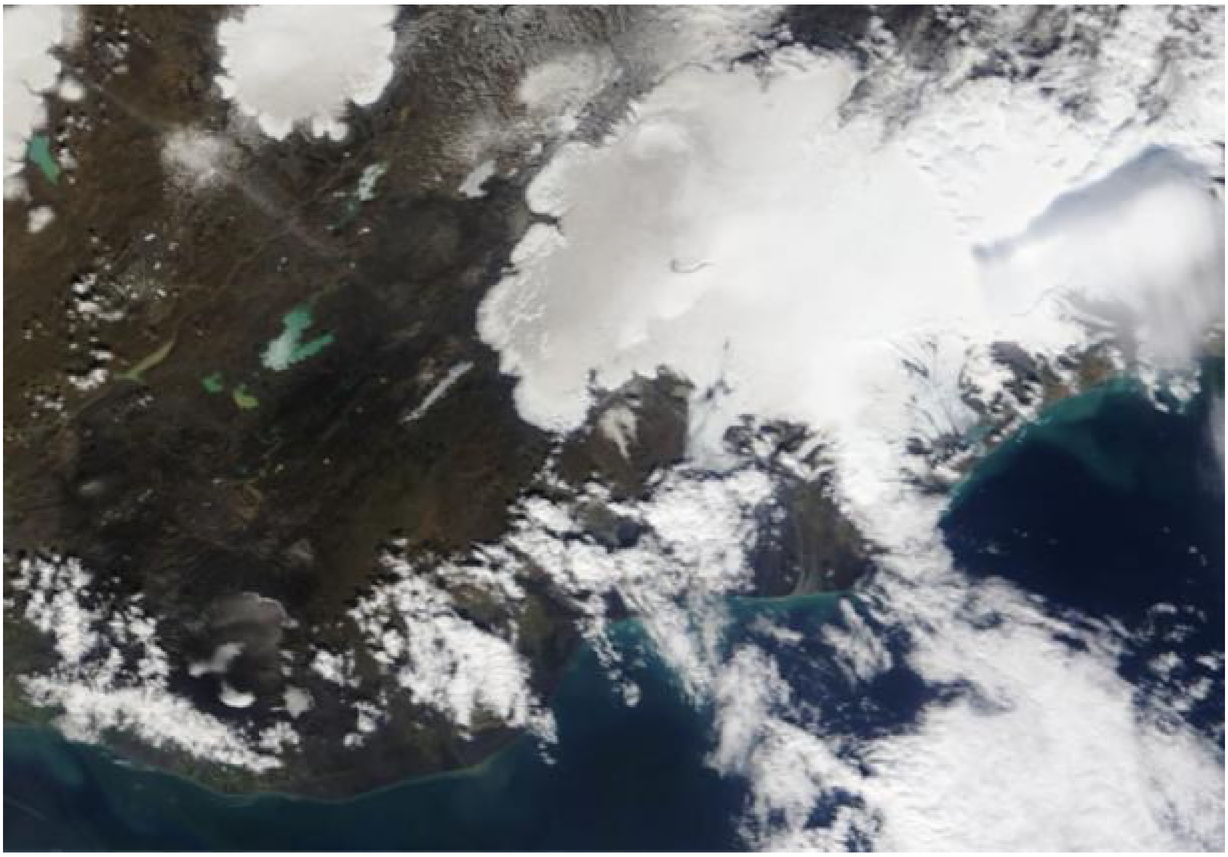

Top: May 28th and bottom May 30th. Significant amount of tephra is visible on western Vatnajökull, Dyngjujökull, Skeiðarárjökull and Breiðamerkurjökull. The darkest areas are south and west of Bárðarbunga. If any, the tephra cover on east and north Vatnajökull is extremely thin. In the first days of June participants in the annual expedition of Iceland Glaciological Society observed high rates of ablation on western Vatnajökull. West of Grímsvötn towards the north the tephra fallout was in metre scale wide bands (with different tephra concentration) of S to N direction. This non-uniform distribution had already melted ½-1 m deep trenches in the first days of June, much of western Vatnajökull was almost impassable.

Left: June 17th 2010; high ablation rates obvious in the tephra covered areas. Right: July 11th, fresh snow in above ~1500 m, the snow line is rushing upwards.

Left: July 21st and right August 11th, the snow line is still rushing upwards on all outlets. The dirt cover on the eastern part may be composed of both tephra and dust from the north highland.

Left: August 27th and right September 13th. The fresh snow seen in the upper regions in August has melted in September. The snow line is still rising.

Left: September 19th, snow is starting to accumulate in the upper regions. Right: October 10th. Winter has settled in, this week the mass balance survey observed up to 120 cm fresh snow at the highest elevations.

The images are either from the MODIS Aqua or MODIS Terra satellites, visible light, 250m resolution.
http://rapidfire.sci.gsfc.nasa.gov/
The Moderate Resolution Imaging Spectroradiometer (MODIS) flies onboard NASA's Aqua and Terra satellites as part of the NASA-centered international Earth Observing System. Both satellites orbit the Earth from pole to pole, seeing most of the globe every day. Onboard Terra, MODIS sees the Earth during the morning, while Aqua MODIS orbits the Earth in the afternoon.

Below MODIS images for all days of May, June, July, August and September 2010 are shown.

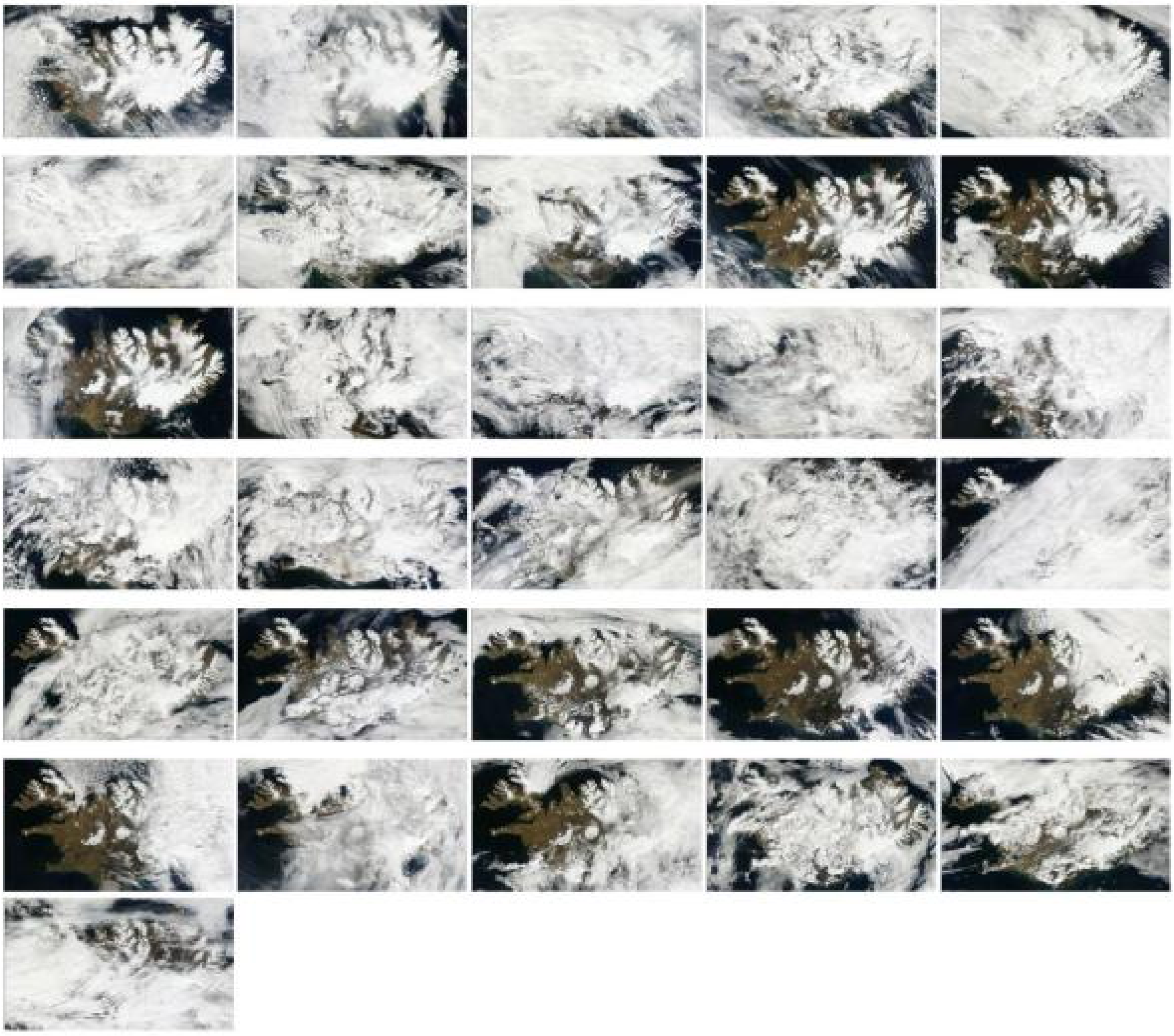

MODIS: May 2010 (read from left to right and downwards).

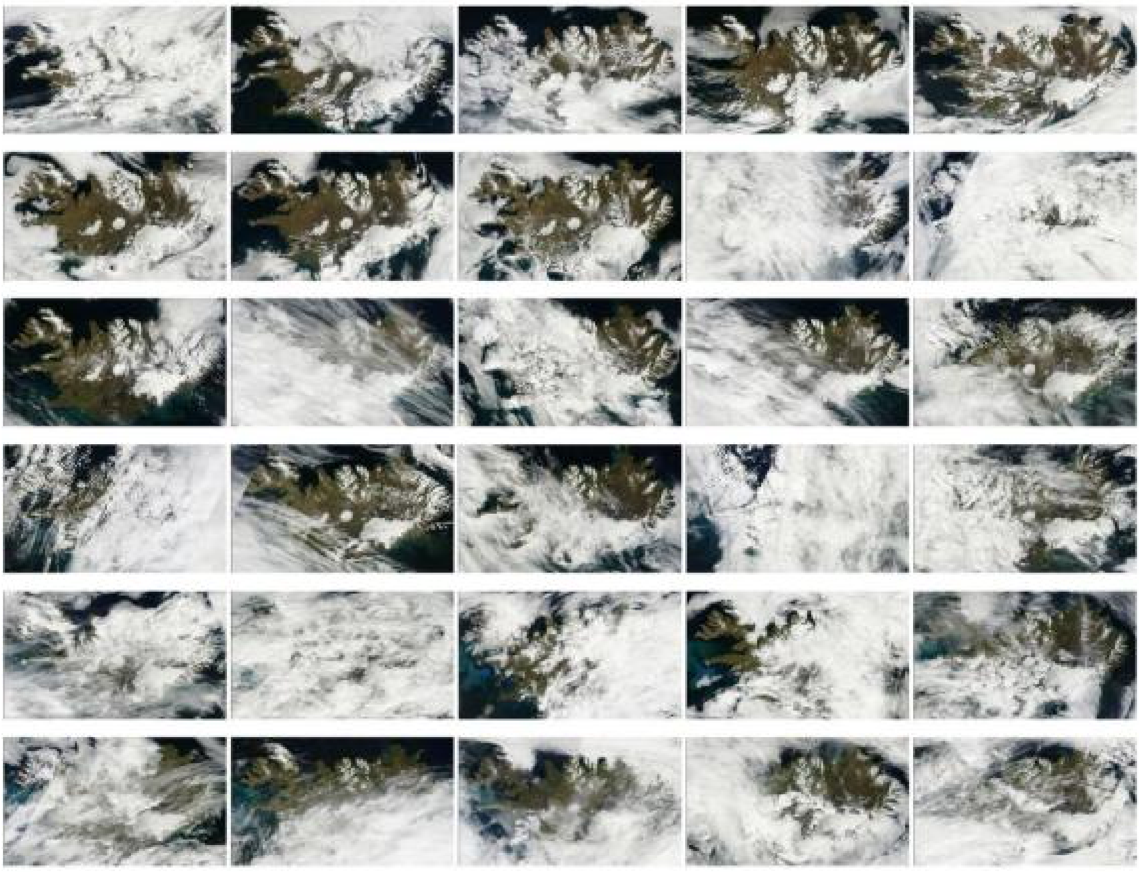

MODIS: June 2010 (read from left to right and downwards).

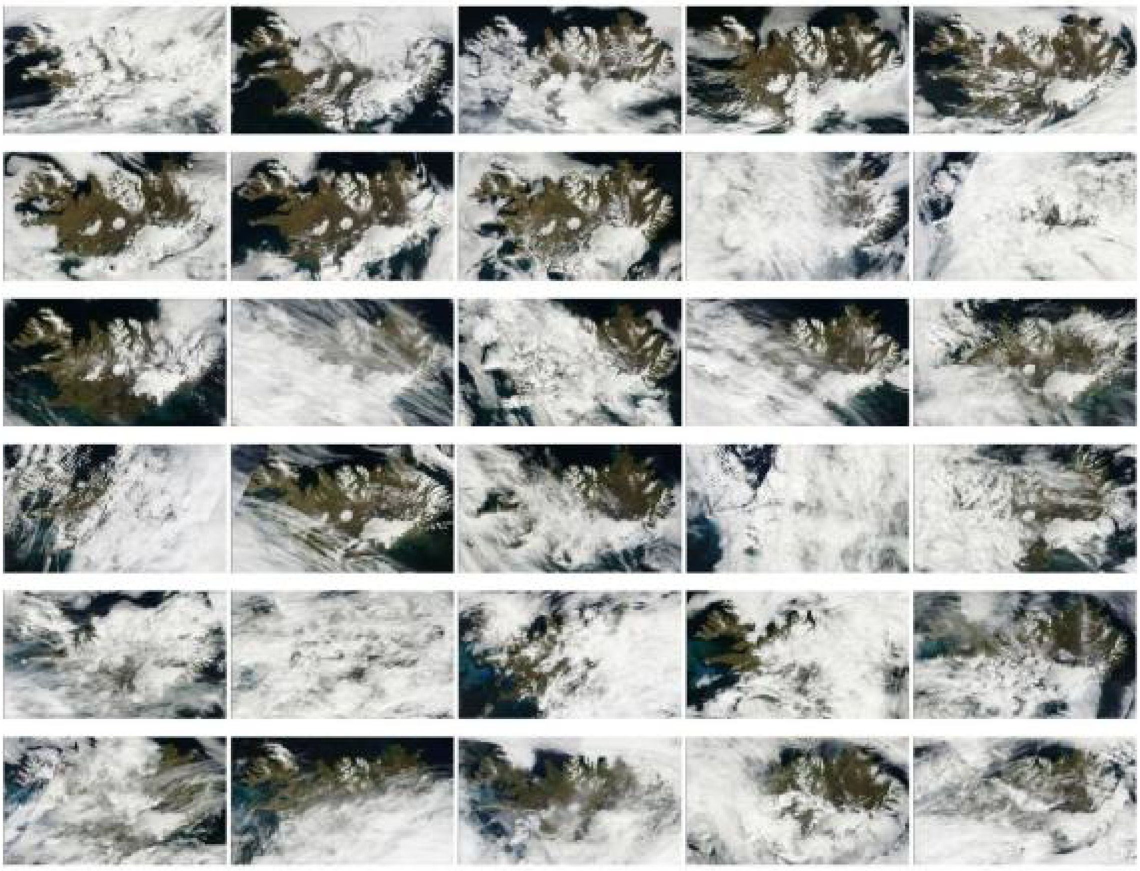

MODIS: July 2010 (read from left to right and downwards).

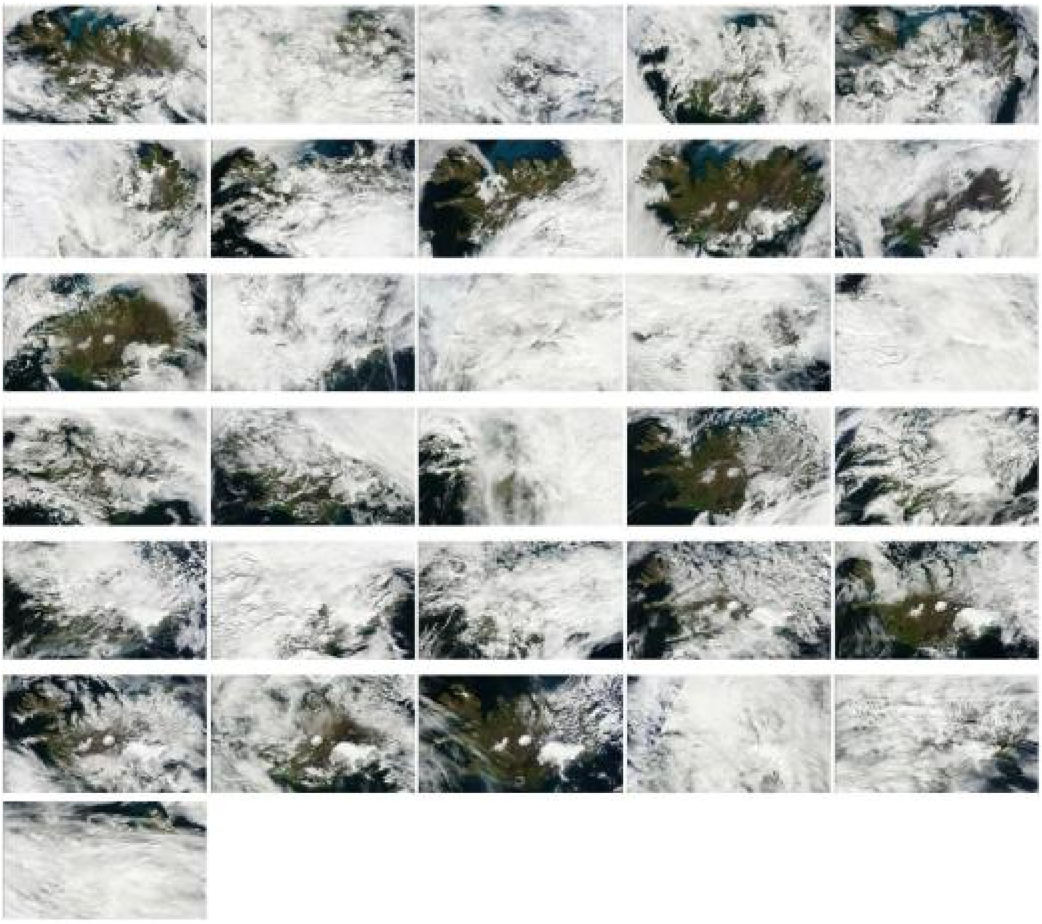

MODIS: August 2010 (read from left to right and downwards).

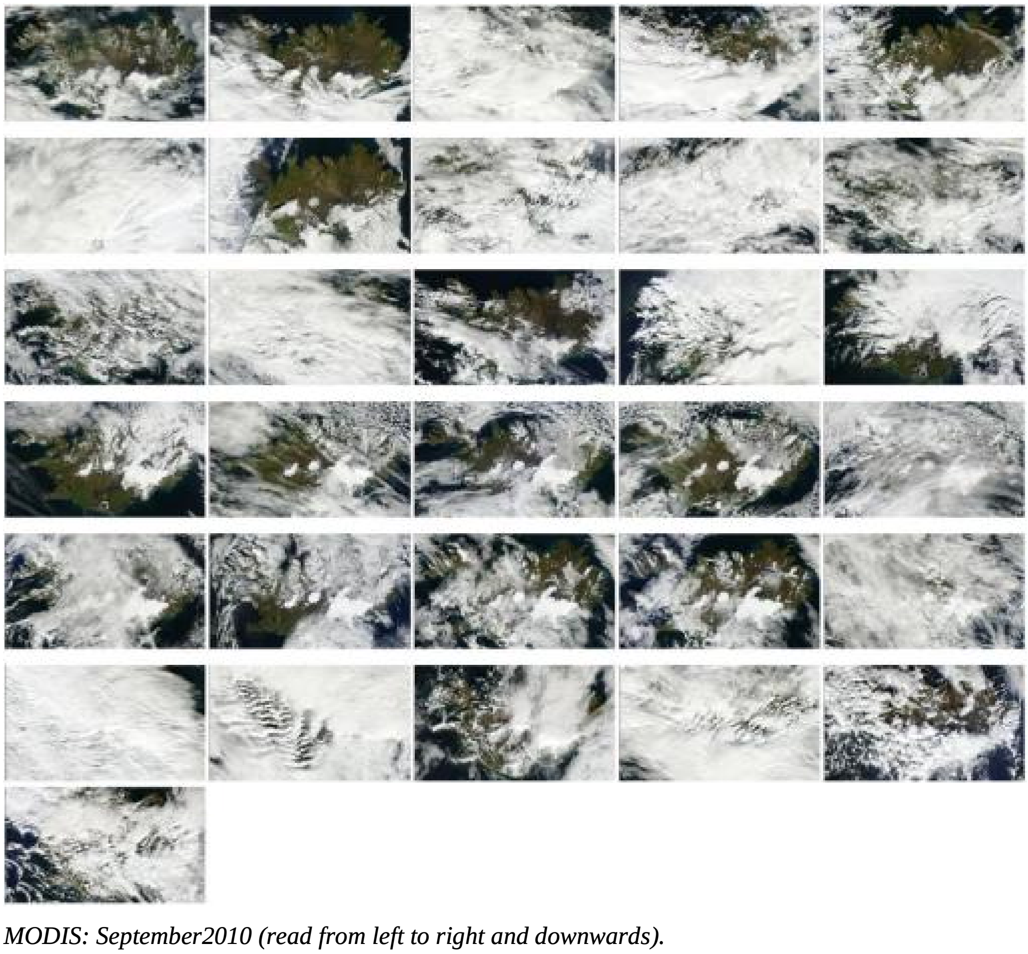

MODIS: September2010 (read from left to right and downwards).